Chapter 5

Structural Insights Into Disease Mutations of the Ryanodine Receptor

Zhiguang Yuchi, Lynn Kimlicka and Filip Van Petegem

Additional information is available at the end of the chapter

http://dx.doi.org/10.5772/53641

1. Introduction

Ca^{2+} ions form important intracellular messenger molecules in nearly every cell type of the human body. Under so-called "resting" states of the cell, the concentration of Ca^{2+} in the cytoplasm is extremely low (~10^{-7}M), but this can rapidly rise ~2 orders of magnitude when an appropriate signal is generated. Ca^{2+} ions can enter the cytoplasm either from the extracellular space or from intracellular compartments, through specialized membrane proteins. These "calcium channels" are complex proteins, often consisting of multiple subunits, and are targets for multiple regulatory events.

A major intracellular Ca^{2+} store is the endoplasmic reticulum (ER), or its specialized form, the sarcoplasmic reticulum (SR) in muscle tissue. The mobilization of Ca^{2+} from these organelles can trigger many Ca^{2+}-dependent events, such as the contraction of muscle tissue. The coupling between electrical excitation of a muscle cell and its subsequent contraction (excitation-contraction coupling, E-C coupling) is a finely orchestrated process that requires a functional cross-talk between proteins embedded in the plasma membrane and in the SR membrane (Figure 1). An electrical signal, a depolarization of the plasma membrane, can lead to opening of L-type voltage-gated calcium channels (Ca_V), which results in the influx of Ca^{2+} into the cytoplasm. In the SR membrane, large calcium release channels called Ryanodine Receptors (RyRs) can detect this initial influx, and release more Ca^{2+} in a process known as Ca^{2+}-induced Ca^{2+} release (CICR). The latter event provides the bulk of the Ca^{2+} required for contraction to occur. In this scenario, the RyRs form signal amplifiers, which both detect and augment the Ca^{2+} signal [1, 2]. This scenario likely predominates in cardiac tissue, but Ca^{2+} is not always required to open RyRs. In skeletal muscle, for example, various pieces of evidence suggest a direct interaction between the L-type calcium channel ($Ca_V1.1$) and the RyR [3-6]. In this case, the depolari-

zation of the plasma membrane causes distinct conformational changes in $Ca_V1.1$, which are then transmitted directly to the RyR, causing them to open.

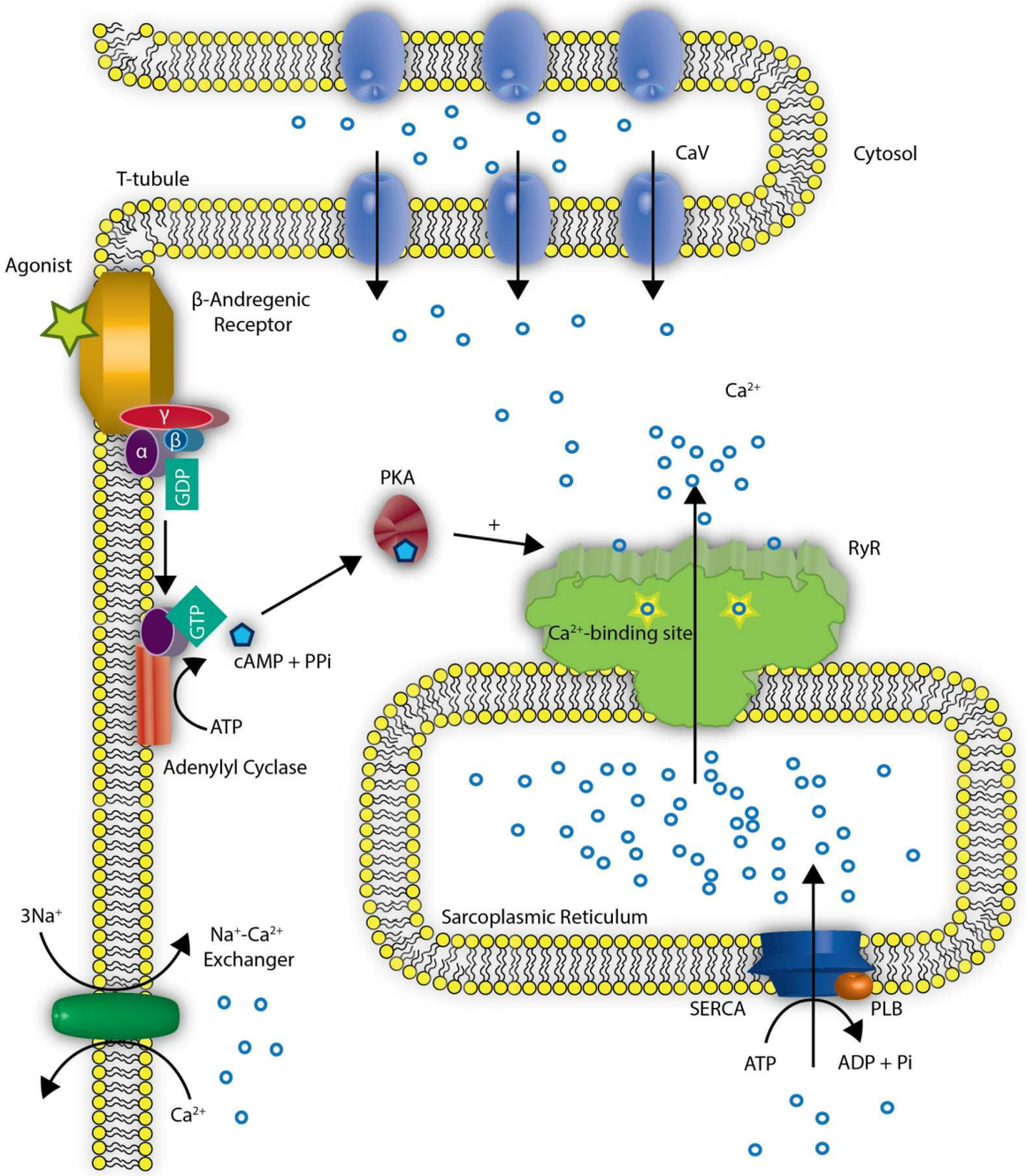

Figure 1. Schematic diagram of components in E-C coupling. Depolarization of plasma membrane (PM) activates the embedded voltage-gated calcium channel (CaV) which conducts Ca^{2+} influx into the cytoplasm. RyRs in SR membrane sense this Ca^{2+} signal and amplify it by releasing more Ca^{2+} from SR store (Ca^{2+} -induced Ca^{2+} release, CICR). This will provide enough Ca^{2+} for the muscle contraction to occur. SERCA pump in the SR and Na^{+}-Ca^{2+} exchanger in the PM pump out the Ca^{2+} from cytoplasm and restore the resting [Ca^{2+}]. The activity of RyR can be upregulated by the PKA phosphoryaltion upon the activation of β-adrenergic receptor on the PM.

http://dx.doi.org/10.5772/53641

RyRs owe their name to the binding of ryanodine, a toxic compound from the South American plant *Ryania speciosa* [7]. RyRs are currently the largest known ion channels, with a massive size of >2.2MDa. They form homotetrameric assemblies [8, 9], and each monomer contains ~5000 amino acid residues. In humans and all other mammalian organisms investigated so far, three different isoforms (RyR1-3) have been found to date. RyR1 is widely expressed in skeletal muscle, and was the first one to be cloned [10, 11]. RyR2 is primarily found in the heart [12, 13] and RyR3 was originally identified in the brain [14], although each isoform is found in many different cell types [15].

Since Ca^{2+} ions form very potent intracellular messenger molecules, it is not surprising that their entry into the cytoplasm is under intense regulation. RyRs therefore form the targets for a plethora of auxiliary proteins and small molecules that are known to regulate their ability to open or close [15-17]. The primary regulatory molecule is cytoplasmic Ca^{2+}, which triggers the channel to open. However, higher Ca^{2+} levels can trigger closing, indicating that there is more than one Ca^{2+} binding site. Under conditions whereby the SR is overloaded with Ca^{2+}, RyRs can also open spontaneously in a process known as store-overload-induced calcium release (SOICR) [18, 19].

An overview of several positive and negative RyR modulators is shown in Figure 2. Well-known regulators include FK506 binding proteins (FKBPs), small proteins that stabilize the closed state of the channels and can prevent the formation of subconductance states [20, 21]. Calmodulin (CaM) is a ~17kDa protein that can bind 4 Ca^{2+} ions in separate EF hands, well-known Ca^{2+}-binding motifs. CaM binds RyR in a 4:1 stoichiometry and can either inhibit or stimulate RyRs depending on the isoform and Ca^{2+} levels [22-25]. RyRs are also the target for several kinases (PKA, PKG, CaMKII) and phosphatases (PP1, PP2A, PDE4D3), and the degree of phosphorylation seems to affect RyR activity [26]. In this chapter, we discuss the involvement of RyRs in several genetic diseases, summarize the outcome of several years of functional studies on disease variants of the RyR, and describe the insights into disease mechanisms through low- and high-resolution structural studies.

2. Ryanodine receptors and genetic disease

2.1. Malignant hyperthermia

Malignant hyperthermia (MH) is a pharmacogenetic disorder, requiring both a genetic mutation and an external trigger to cause a disease phenotype. The condition is mostly linked to mutations in the RyR skeletal muscle isoform (RyR1), but some mutations in the skeletal muscle L-type calcium channel ($Ca_V1.1$) can also cause MH [27]. It is typically triggered by the use of inhalational anesthetics or succinylcholine, a muscle relaxant [28]. The condition is considered rare, with an incidence of 1:60,000 for adults or 1:15,000 for children [29]. An MH episode is characterized by an abnormal rise in the core body temperature, skeletal muscle rigidity, acidosis, and tachycardia. Most modern surgery rooms monitor for these signs, and will make use of dantrolene, which can rapidly reverse the symptoms. Dantrolene acts by decreasing the intracellular Ca^{2+} concentration [30]. Several studies suggest a direct interac-

tion between dantrolene and RyR1, and it is thought that dantrolene directly prevents Ca^{2+} release through RyR1 [31, 32].

The first link between MH and RyR1 came through a related disorder in pigs, known as porcine stress syndrome (PSS). It was found that the pig RyR1 mutation R615C underlies PSS [33], and soon after the corresponding mutation in humans was linked to MH [34].

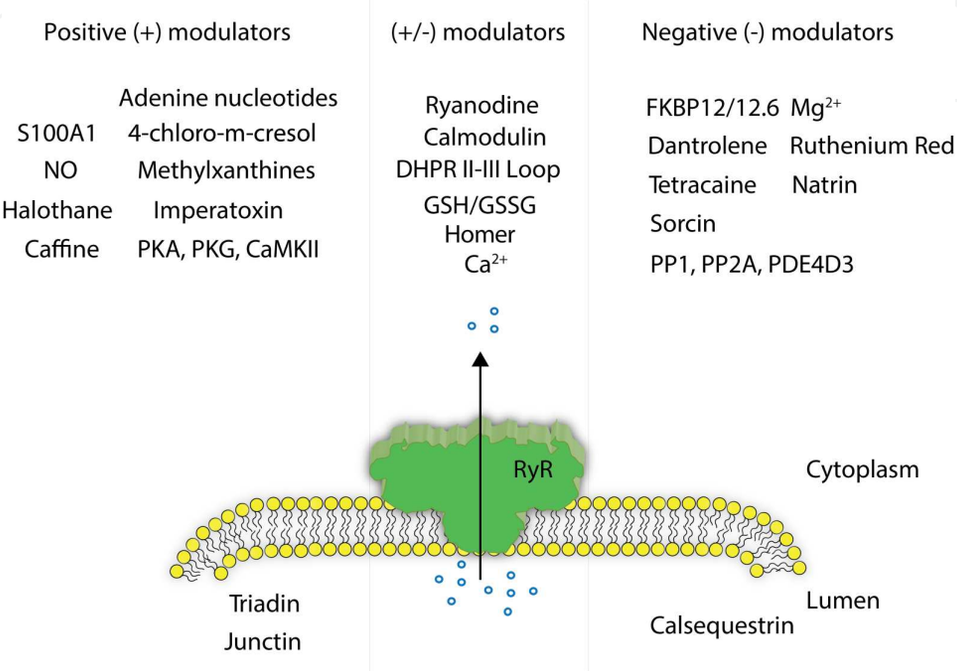

Figure 2. Regulation of RyRs. RyRs are regulated by a number of postive and negative modulators from both the cytoplasmic and SR luminal sides. S100A1: S100 calcium-binding protein A1; NO: nitric oxide; PKA: cAMP-dependent protein kinase; PKG: cGMP-dependent protein kinase; CaMKII: Ca^{2+}/calmodulin-dependent protein kinase II; DHPR: dihydropyridine receptor/L-type voltage-dependent calcium channel; GSH: glutathione; GSSG: glutathione disulfide; FKBP12/12.6: FK506 binding protein 12/12.6; PP1: protein phosphatase 1; PP2A: protein phosphatase 2; PDE4D3: cAMP-specific 3',5'-cyclic phosphodiesterase 4D3.

2.2. Core myopathies

Central core disease (CCD) is a congenital myopathy, characterized by progressive muscle weakness and the presence of metabolically inactive tissue (cores) in the center of muscle fibers. These cores lack mitochondria and the myofibrillar organization is disrupted. The common phenotype of CCD includes muscle atrophy, floppy infant syndrome and skeletal muscle deformities [35, 36]. It was found early on that there is a connection between CCD and MH susceptibility [37], and some RyR1 mutations have been found to cause both. Multi-mini core disease (MmD) is another inherited congenital myopathy. Different from CCD, whose inheritance is autosomal dominant, MmD is usually considered recessive [35]. As its name suggests, MmD is characterized by the presence of multiple not-well-defined cores in muscle fibers. MmD can cause axial muscle weakness that can lead to severe scoliosis [35]. Although MmD is mainly associated with mutations in RyR1 [38], mutations in selenopro-

tein N 1 [39], a protein required for RyR1 calcium release [40], and α-actin (ACTA1) [41] have also been found to underlie MmD.

2.3. Catecholaminergic polymorphic ventricular tachycardia

Also known as CPVT, this disorder manifests itself in young individuals, with either syncope or sudden cardiac death as the first symptom. Many affected individuals will develop cardiac arrhythmias that are triggered by exercise or emotional stress. CPVT is mostly detected through stress tests, which indicate bidirectional ventricular tachycardia. Typically no morphological abnormalities of the myocardium are detected. The disease is mostly due to mutations in the cardiac RyR2 isoform [42], but mutations in the associated proteins calsequestrin [43] and triadin [44] can also be the cause. As CPVT is triggered by β-adrenergic stimulation, it can be treated by β-blockers [45]. Flecainide, a sodium channel blocker, has also been found to be beneficial for CPVT patients [46].

Now more than 20 years since the initial identification of the first RyR disease mutations, nearly 500 mutations have been found in RyR1 and RyR2 combined. In RyR1, most disease mutations seem to be spread across the gene, with some clustering in distinct areas, whereas in RyR2, most mutations are found in one of 3 or 4 different disease hot spots (Figure 3). The appearance of clusters may be due to bias in sequencing, as historically only the areas that had already shown to be involved in disease were being considered for sequence analysis.

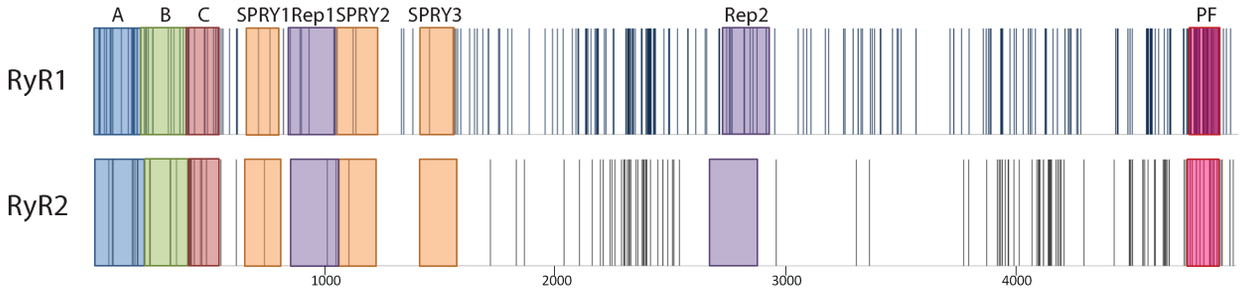

Figure 3. Disease hot spots. Linear view of the RyR1 and RyR2 sequences with each vertical line representing a disease mutation. The areas of solid colors correspond to domains A(blue), B (green), C (red), SPRY (orange), Tandem Repeat domains (Rep) (purple) and Pore-forming domain (PF) (pink).

3. Functional studies

Although increasing numbers of RyR mutations are identified in patients and their family members, only a handful of them have been validated as causative disease mutations [29]. Functional studies are necessary to prove the molecular basis of the mutations as pathogenic. Without functional characterizations, the possibility that the mutations are the result of polymorphism cannot be ruled out. In this section, different methods of performing functional studies and their results are highlighted.

3.1. Model systems

There are a variety of ways to prepare model systems to study functional effects of mutations in RyRs: endogenous or recombinant expression systems and *in vivo* models.

In the early days, before and shortly after the discovery of RyR mutations in MH-susceptible pigs and individuals, SR vesicles were prepared from muscle biopsies [47-55]. SR vesicles from non-MH-susceptible animals or individuals were also obtained to serve as controls. These are endogenous expression systems since SR vesicles contain RyRs, and therefore, can be used as a whole or can be further purified to obtain single RyR channels. These approaches can be invasive, as they involve acquisition of native RyRs expressed in patients or knock-in mice carrying mutations. For example, skeletal myotubes have been isolated from MH-susceptible and/or CCD patients [56-59]. Both RyR1 and RyR2 can be studied by isolating skeletal myotubes and cardiomyocytes from knock-in mice, respectively [60-73]. Flexor digitorum brevis fibers, present in the feet, have also been derived from knock-in mice for the study of RyR1 mutations [67, 74-76]. In some cases, measures have been taken to alleviate some of the affliction on obtaining native RyRs from patients by using less invasive approaches. In one study of a CCD-associated RyR1 mutation, fibroblasts from a CCD patient were differentiated into muscle by myoD conversion with adenovirus [77]. In other cases, immortalized lymphoblastoid cells were generated using B-lymphocytes isolated from blood samples [78-83].

A more commonly used model is a recombinant expression system. By using cells that lack the native expression of RyRs, all results will arise only from the mutant RyR. One of the most commonly used systems are dyspedic myotubes, which are derived from mice that lack RyR1, called "RyR1-null mice" [80, 84-90]. Also commonly used are human embryonic kidney (HEK)-293 cells. HEK-293 cells not only lack native RyR expression but also lack other complexes involved in E-C coupling and yet have been demonstrated to express functional RyR when its cDNA is transfected [19, 79, 80, 89-115]. Other cell lines used in functional studies include COS-7 [116], myoblastic C_2C_{12} [117], HL-1 cardiomyocytes [108, 110, 115, 118], and CHO cells [119].

Finally, knock-in mice have served as valuable models for the study of mutations in RyR1 and RyR2 [60-64, 66-76, 120-128]. The comparison between mice that are homozygous or heterozygous for the mutation in question has provided clues about the gene dosage effects. Studying the effect of mutations on the body as a whole provides insights that are more relevant to clinical phenotypes.

3.2. Methods

Multiple techniques have been implemented to study mutant RyRs from different expression systems. Five major methods are introduced here.

One way to measure Ca^{2+} release through RyR channels is through [$^{45}Ca^{2+}$]-uptake and -release assays [50, 52, 98]. Microsomal vesicles expressing recombinant RyR and SERCA1a are prepared. The vesicles are then incubated with $^{45}Ca^{2+}$, during which SERCA1a pumps $^{45}Ca^{2+}$ into the vesicles. By comparing the amount of $^{45}Ca^{2+}$ accumulation in the presence

http://dx.doi.org/10.5772/53641

or absence of the potent RyR inhibitor Ruthenium Red, the amount of Ca^{2+} release through RyR can be determined.

A more widely used technique is a Ca^{2+} fluorescence assay involving whole cell samples (Figure 4A,B) [19, 57-59, 70, 71, 73, 77, 79, 89, 91-93, 95, 102, 104-106, 108, 109, 112, 113, 115-118]. Cells with either endogenous or recombinant expression of RyR are loaded with a fluorescent Ca^{2+} indicator, such as fura-2, which diffuses throughout the cytoplasm. By measuring fluorescence with confocal microscopy, resting [Ca^{2+}] levels in the cytoplasm, as well as frequency, duration, and extent of Ca^{2+} release from RyR can be calculated.

Commonly used is a [^{3}H]ryanodine binding assay (Figure 4C) [19, 51, 54, 60, 67, 77, 79, 86, 90, 92, 93, 95, 96, 103, 105, 108, 113, 129]. SR vesicles containing endogenous or recombinant RyR are incubated with radioactive [^{3}H]ryanodine. Since ryanodine binds to the channels in the open state, binding of [^{3}H]ryanodine is indicative of the measure of open channels. The extent of RyR activation is then measured by radioactive counting.

As opposed to whole-cell measurements, activities of a single channel can be recorded using planar lipid bilayer electrophysiology (Figure 4D) [19, 53, 54, 67, 69, 77, 79, 99-101, 105, 107, 108, 111, 112, 114]. Recombinant or endogenous RyR from crude SR vesicle preparations or from purified material are fused into an artificial lipid bilayer formed across two chambers. The current generated by ions passing through the channel is recorded. This method allows various properties of the single channel to be determined, including the open probability, duration of the open and closed time, and conductance. The two chambers can resemble cytoplasmic and luminal sides of the channel, allowing the studies of Ca^{2+}-induced Ca^{2+} release (CICR) from the cytoplasmic side or store-overload-induced Ca^{2+} release (SOICR) from the luminal side. The planar lipid bilayer technique also allows for additional control because purified auxiliary proteins or pharmacological modulators can be added to either side.

3.3. Highlight of the results

Functional studies of mutant RyR channels have generated multitudes of insights into the molecular basis of the RyR channelopathies. Accordingly, complex sets of results have been generated that require careful interpretation and have resulted in a lot of debate. For example, many mutations seem to make the RyR channels more active, but the exact nature of this change is still under scrutiny. In some cases, mutations seem to be more sensitive to cytosolic activators, while other evidence suggests they are more sensitive to luminal Ca^{2+} levels. Others suggest that altered phosphorylation states of the channel or affinity to auxiliary proteins is the causative mechanism. For this section, results of the functional studies are highlighted as mutations that cause RyRs to be either hypersensitive (more prone to open upon stimulation) or hyposensitive (requiring more stimulus to open). RyR mutations can be pathogenic either through hyper- or hypo-activity since alteration in Ca^{2+} homeostasis in either direction can cause aberrant muscle functions. Yet other mutations have exhibited no apparent alterations in the functional studies performed so far. The results are summarized in Table 1.

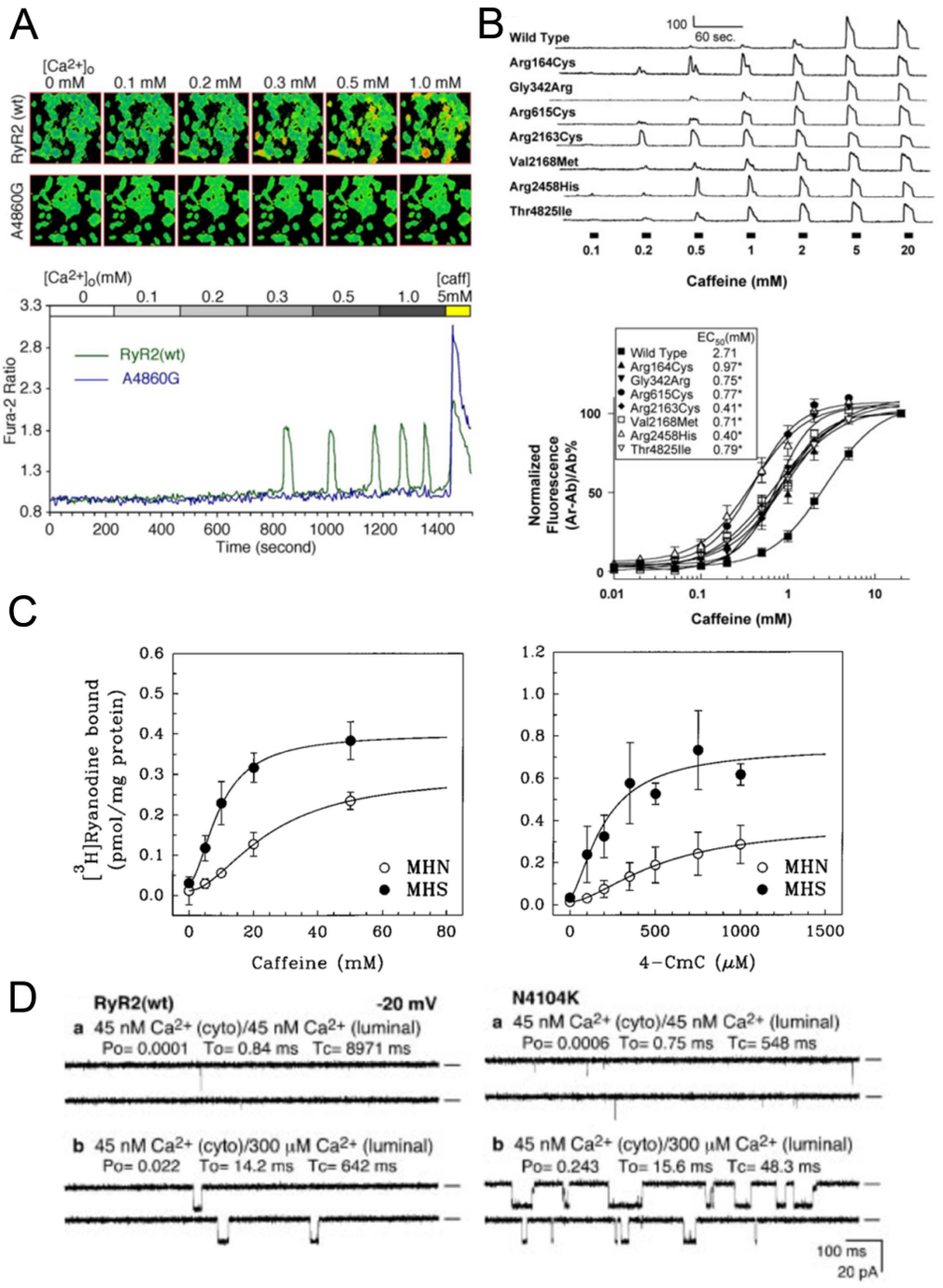

Figure 4. Representative figures from exemplary functional studies. (A) Single-cell fluorescent Ca^{2+} images of HEK-293 cells expressing RyR2 WT and A4860G at various extracellular [Ca^{2+}] (*top*) and fura-2 ratios of representative RyR2 WT and A4860G cells (*bottom*)[110]. (B) Representative single-cell fluorescent traces of Ca2+ release stimulated by incremental doses of caffeine in dyspedic myotubes transfected with RyR1 WT and mutants cDNAs (*top*) and corresponding sigmoidal dose-response curves (*bottom*)[86]. (C) [^{3}H]ryanodine binding assay on SR vesicles from MHN (malignant-hyperthermia non-suceptible, or RyR1 WT) and MHS (malignant-hyperthermia suceptible, or RyR1 G2434R) individuals in presence of caffeine (*left*) and 4-CmC (*right*)[55]. (D) Single-channel activities of RyR2 WT and N4104K recorded in planar lipid bilayers with luminal [Ca^{2+}] of 45nM (*a*) or 300nM (*b*). Downward strokes in the current traces denote channel-opening events[19].

http://dx.doi.org/10.5772/53641

Effect	Isoform	Mutations	Disease	References	Mutations	Disease	References
Hyperactive	RyR1	C35R	MH	[91, 94]	R2355W	MH	[58]
		R163C	MH/CCD/MmD	[61, 65-67, 85, 86, 91, 94, 103]	E2371G	MH	[82]
					G2375A	MH	[58]
		G248R	MH	[91, 94, 103]	G2434R	MH	[1,2,36]
		R328W	MH	[97]	R2435H	MH/CCD	[85, 91, 94]
		G341R	MH	[86, 91, 94]	R2435L	MH/CCD	[77, 88]
		H382N	MH	[83]	I2453T	MH/CCD	[57]
		I403M	MH/CCD	[91, 94]	R2454H	MH/CCD	[82]
		Y522S	MH/CCD	[60, 63, 64, 85, 87, 89, 91, 94, 120]	R2458C	MH	[91, 94]
					R2458H	MH	[86, 91, 94]
		R530H	MH	[82]	R2458H/R3348C	MH	[59]
		R552W	MH	[91, 94]	R2508C	MH/CCD	[102]
		A612P	MH	[59]	R2508G	MH	[83]
		R614C	MH	[47-52, 54, 86, 88, 89, 91, 94, 101, 116, 117, 129]	ΔR4214_F4216	CCD	[80]
					T4637A	CCD	[88]
		R614L	MH	[91, 94]	Y4796C	CCD	[87, 88]
		E1058K	MH	[83]	T4826I	MH	[76, 86, 103, 122]
		K1393R	MH	[83]	H4833Y	MH	[81, 103]
		R1679H	MH	[83]	R4861H	CCD	[78]
		R2163C	MH	[86, 88, 91, 94]	ΔF4863_D4869	CCD	[79]
		R2163H	MH/CCD	[85, 88, 91, 94]	R4893W	CCD	[78]
		R2163P	MH	[82]	A4894T	MH	[104]
		V2168M	MH	[86]	I4898T	CCD	[78, 89, 93]
		T2206M	MH	[56]	G4899R	CCD	[78]
		N2283H	CCD/MmD	[99]			
		N2342S	MH	[82]			
		ΔE2347	MH	[88]			
		A2350T	MH	[58, 96]			
	RyR2	ΔExon 3	CPVT	[115]	N2386I	ARVD2	[106, 109]
		A77V	CPVT/ARVD2	[115]	R2474S	CPVT	[48,125,54]
		R176Q	ARVD2	[106, 126-128]	T2504M	ARVD2	[106]
		R176Q/T2504M	ARVD2	[108, 109, 112, 115]	N4104K	CPVT	[19, 118, 119]
		E189D	CPVT	[113]	Q4201R	CPVT	[107, 108, 112]
		G230C	CPVT	[114]	R4497C	CPVT	[19, 68, 71, 72, 105, 118, 119, 123, 124]
		R420W	ARVD2	[115]			
		L433P	ARVD2	[108, 109, 115]	S4565R	CPVT	[111]
		S2246L	CPVT	[48,50,56-58]	V4653F	CPVT	[107, 112]
		R2267H	CPVT	[111]	I4867M	CPVT	[108]

Effect	Isoform	Mutations	Disease	References	Mutations	Disease	References
		P2328S	CPVT	[52, 54, 55]	N4895D	CPVT	[19]
Hypoactive	RyR1	S71Y/N2283H	CCD/MmD	[99]	I4898T	CCD	[7,12,13,46,70,73,74, 75]
		R109W/M485V	CCD/MmD	[99, 100]	G4899R	CCD	[87, 100, 103]
		C4664R	MH	[82]	G4899E	CCD	[98, 100]
		G4891R	CCD	[87]	A4906V	CCD	[87]
		R4893W	CCD	[87, 98]	R4914G	CCD	[87]
		A4894P	CNMDU1	[104]	ΔV4927_I4928	CCD	[80, 100]
	RyR2	L433P	ARVD2	[106]	A4860G	IVF	[110, 112]
		A1107M (T1107M)	CPVT	[115]			
Uncertain effects	RyR1	I403M A1577T/ G2060C	MH/CCD	[85]	G3938A (G3938D)	MH	[95]
			CCD	[99]		MH	[92]
		R2939K	MmD	[90]	D3986A (D3986E)		
	RyR2						

Table 1. Summary from functional studies on RyR disease-associated mutations. Mutations that alter RyR functions are listed as hyperactive or hypoactive. Mutations with no discernable change compared with wild type channel are listed as "uncertain." References to the functional studies are listed beside the corresponding mutations. (Δ) = deletion mutation. (/) = double mutation. Amino residue numbering is for human RyRs. (MH) = Malignant hyperthermia, (CCD) = central core disease, (MmD) = multi-minicore disease, (CNMDU1) = congenital neuromuscular disease with uniform type 1 fiber, (CPVT) = catecholaminergic polymorphic ventricular tachycardia, (ARVD2) = arrhythmogenic right ventricular dysplasia type 2, and (IVF) = idiopathic ventricular fibrillation.

The majority of the mutations in both RyR1 and RyR2 have been shown to make the channels hyperactive. This includes the first disease-associated mutation found in porcine stress syndrome, RyR1 R615C. Functional studies have revealed that RyR1 channels with this mutation have significantly lowered threshold for activation by [Ca^{2+}], caffeine, and halothane compared to wild-type channels, while having markedly increased threshold for inactivation by [Ca^{2+}], Ruthenium Red, or Mg^{2+} ions [47-52, 101, 116, 117, 129]. These results are characteristic of mutations that alter RyRs into hypersensitive channels [19, 55-59, 61, 63, 65, 67-69, 71, 73, 76-83, 85-89, 91, 93, 94, 96, 97, 102-109, 111-115, 118, 119]. RyRs that are hyperactive are often described as "leaky," and on top of their increased sensitivity towards activators or reduced sensitivity towards inhibitors, they often exhibit increased resting [Ca^{2+}] in the cytoplasm, reduced SR Ca^{2+} store content, or altered maximal Ca^{2+} release.

Although less common, some mutations in RyR have been demonstrated to reduce channel activity. [62, 74, 75, 80, 82, 84, 87, 89, 98, 100, 103, 104, 106, 110, 112, 115]. For example, the I4898T mutation in RyR1, associated with an unusually severe and highly penetrant form of CCD, has been shown to cause complete uncoupling of sarcolemmal excitation from SR Ca^{2+} release, in which activating signals from L-type Ca_V channels to RyR1 are uncoupled [84]. It has also been shown that the I4898T mutation leads to a complete loss of Ca^{2+} release induced by caffeine stimulation [89]. Many other CCD-associated mutations that are located at the predicted pore region of RyR1 (G4890R, R4892W, A4894P,

I4897T, G4898R, G4898E, A4905V, and R4913G) have also been shown to abolish E-C coupling and/or exhibit reduced sensitivity to activation by [Ca^{2+}], caffeine, or 4-CmC [62, 87, 98, 100, 103, 104]. Mutations that disrupt signaling between the L-type Ca_V and RyR are known as "E-C uncoupling" mutations. In RyR2, fewer mutations have thus far been associated with a reduction in activity, suggesting that a loss of function in RyR2 may be less tolerated than in RyR1. The A4860G mutation in RyR2 is associated with idiopathic ventricular fibrillation (IVF) and is located at the predicted inner pore helix. It has been shown to diminish response or increase the threshold for activation by SOICR [110, 112]. Furthermore, the mouse RyR2 A1107M mutation (corresponding to the T1107M mutation that is associated with hypertrophic cardiomyopathy in humans) has been shown to increase the threshold for Ca^{2+} release termination [115].

Effects of some other disease-associated mutations are less apparent. For instance, single channel measurements of RyR1 A1577T and G2060C mutant channel produced no discernible change in the activity of the channel compared to wild type [99]. Similarly, [^{3}H] ryanodine binding assays of RyR1 R2939K expressed in HEK-293 cells failed to show alteration in Ca^{2+} dependence and caffeine activation compared to wild-type channel [90]. In addition, RyR1 I404M expressed in dyspedic mice myotubes exhibited resting [Ca^{2+}] levels and SR Ca^{2+} content comparable to that of the wild type [85]. Furthermore, expressions of RyR1 D3987A and G3939A rabbit cDNA in HEK-293 cells, which correspond to the positions of MH-associated mutations D3986E and G3938D in humans, respectively, showed responses to activation by [Ca^{2+}], caffeine, and 4-CmC comparable to that of wild type [92, 95]. For these mutations where no clear functional effect has been observed, it is of course possible that they are not causative of the disease but, instead, simply represent polymorphisms. Alternatively, their effect may only become apparent in the native context, where particular regulatory mechanisms exist that are not captured by the model systems.

Overall, there is an apparent theme between RyR activity and disease phenotype. MH and CPVT are associated with RyRs that have an overall gain-of-function phenotype. On the other hand, CCD can be due to either a gain or a loss of RyR1 activity. Loss of function results in impaired Ca^{2+} release, and hence decreased contractility observed in CCD. The gain of RyR1 activity can lead to a general "leak" of Ca^{2+}, resulting in an overall lowered concentration of Ca^{2+} in the SR. The result is then an insufficient amount of Ca^{2+} being available for an E-C coupling event, again resulting in decreased contractility.

For those mutations with less clear effects, as well as those which have been shown to be causative for aberrant Ca^{2+} homeostasis, combining functional studies with structural investigations would provide further useful insight into the molecular basis of disease-associated mutations in RyRs.

4. Structural studies of RyRs

Structural biology has thrived in recent decades and provides researchers with powerful tools for exploring all aspects of life. Different structural techniques, covering the resolution

range from 50 Å down to 1 Å, can reveal the structural details of various bio-molecules, from large protein/DNA/RNA complex to small peptides, which help to improve our understanding of the physiology and pathology of many biological systems.

However, the large size of the RyR and its membrane protein nature make it a very challenging target for structural studies. Most structural techniques require protein samples with high yield and purity, which is normally achieved by overexpression in recombinant systems combined with multi-step chromatography purification processes. The large size of the RyR makes the recombinant expression difficult because the folding of this giant requires the assistance of many chaperones which are often absent in non-native expression systems. The differences in the protein trafficking and post-translational modification systems may also affect the maturation of the recombinant RyR. The alternative way is to purify RyRs from native tissues, but the purification is not easy without artificial affinity tags. To further complicate the issue, the presence of a large exposed hydrophobic surface in the transmembrane region requires the addition of detergents to make the protein soluble during the purification. The denaturing property of the detergents usually makes the sample less homogenous and their presence also affects the crystal packing, both of which are undesirable for x-ray crystallography. The intrinsic dynamic feature of this multi-domain channel further increases heterogeneity of the sample and makes it harder to study.

Despite all the technical difficulties, during the last two decades, several structures of RyRs have been obtained using cryo-electron microscopy (cryo-EM) [130-141], NMR [142] and X-ray crystallography [143-148]. Some of these structures [142, 143] describe how regulatory proteins interact with small fragments (peptides) from RyRs and are not relevant to the theme of this book. Here we will focus on the structures of the full-length channel or large domains where disease mutations are localized, and show how the structural studies can reveal the molecular mechanism of a genetic disease. More details on the structural insights into RyR function have been described in a recent review paper [149].

4.1. Cryo-EM studies of RyRs

Electron microscopy has been able to obtain structural information on RyRs at near sub-nanometer resolution. The early studies using thin-section or negative stain electron microscopy discovered some "feet" structures (square-shaped densities) in the junction region between the SR and T-tubules in muscle tissues [150-157]. The identities of these "feet" were confirmed later when the purified RyRs were imaged by EM, showing similar densities [9]. The negative stain structures with improved resolution revealed that RyRs have a four-fold symmetry and can interact with four neighbouring molecules to form two-dimensional checkerboard-like lattices both in native tissue and in vitro [158-162], suggesting that RyRs may interact cooperatively during gating. The resolution was further improved by the cryo-EM technique [130-141], in which the protein samples are studied under cryogenic temperatures. So far the highest resolution reaches 9.6 Å for RyR1 in a reported closed state.

Many structural details can be appreciated from the cryo-EM structures. The overall shape of the RyR is like a mushroom with a large cap in the cytoplasmic domain (27 × 27 × 12 nm) and a small stem (12 × 12 × 6 nm) crossing the ER/SR membrane. Instead of

http://dx.doi.org/10.5772/53641

a single rigid block, the large "cap" consists of fifteen individual globular regions per subunit with many solvent channels in between [163, 164] (Figure 5A,B). This arrangement maximizes the total exposed surface area, and RyRs thus form perfect scaffolds for many small molecules and protein regulators to dock. The number of transmembrane (TM) helices in the "stem" is still controversial at the current resolution. Five or six TM helices can be detected in the cryoEM maps [134, 141], but it has been suggested that the total number should be either 6 or 8 [165]. The last two TM helices create the pore-forming domain, which is homologous to the ones from tetrameric potassium channels and bacterial sodium channels [141].

Comparison of the RyR structures in the closed and open states reveals movement in both the "cap" region and "stem" region upon channel gating. An iris-like movement around the pore switches the channel between dilated and constricted conformations [166] (Figure 5C,D). Samso *et al.* systematically produced RyR structures in the closed and open states and found the inner helices in the TM region to kink in the open state, increasing the diameter of the pore by ~4 Å [132]. However, another group reported that the inner helics are already kinked in the closed state [141]. The discrepancy can be attributed to differences in sample preparation. Although the conditions may favor a closed or open channel when the RyR is in a membrane, this may not be the case after extraction with detergents. In addition, the amount of oxidation in the sample can also affect the open probability of the channel. It is therefore possible that the 9.6Å map represents an open, rather than a closed channel, and this would reconcile the discrepancies between both studies. So far, most cryo-EM studies are done on RyR1 due to its relatively high abundance. RyR2 and RyR3 have also been studied via cryo-EM [137, 138], albeit at lower resolution. The overall folding is similar for all three isoforms. The major difference between RyR1 and RyR2 is the clamp region on the corner of the "cap" [138], while a central domain (possibly corresponding to the residues 1303-1406 in RyR1), which is missing in RyR3, is the most divergent part between RyR1 and RyR3 [137]. These structural elements very likely contribute to the different properties of the three subtypes.

The cryo-EM studies of RyRs thus far do not provide the resolution to locate individual residues as X-ray crystallography does, but it can give clues about the approximate locations of individual domains through analysis of the difference densities from insertion of fusion proteins (such as GFP) or binding of antibodies for the particular domain. The locations of the three disease hot spots have drawn particular interest since these parts are certainly important for channel function, as the clustering of disease-associated mutations suggests. From the primary sequence analysis, it is clear that the third hot spot is in the transmembrane region ("stem") of the channel. Several insertion studies localize the N-terminal disease hot spot at the clamp region between the subdomain 5 and 9 [31, 167-169], and the central hot spot between the subdomain 5 and 6 [170], suggesting that these two hot spots interact with each other [171] (Figure 5A,B). Similar methods were also used to localize the divergent regions [172-176] and the phosphorylation sites [177, 178]. The accuracy of these studies varies depending on the resolution, linker length, insertion site selection and the size of the fusion protein or antibody. Difference densities analysis was also used to identify the binding sites

of protein regulators, such as FKBP12/12.6 [133, 179-181], calmodulin [180, 182, 183], chloride intracellular channel 2 (CLIC-2) [184] and various toxins [185, 186].

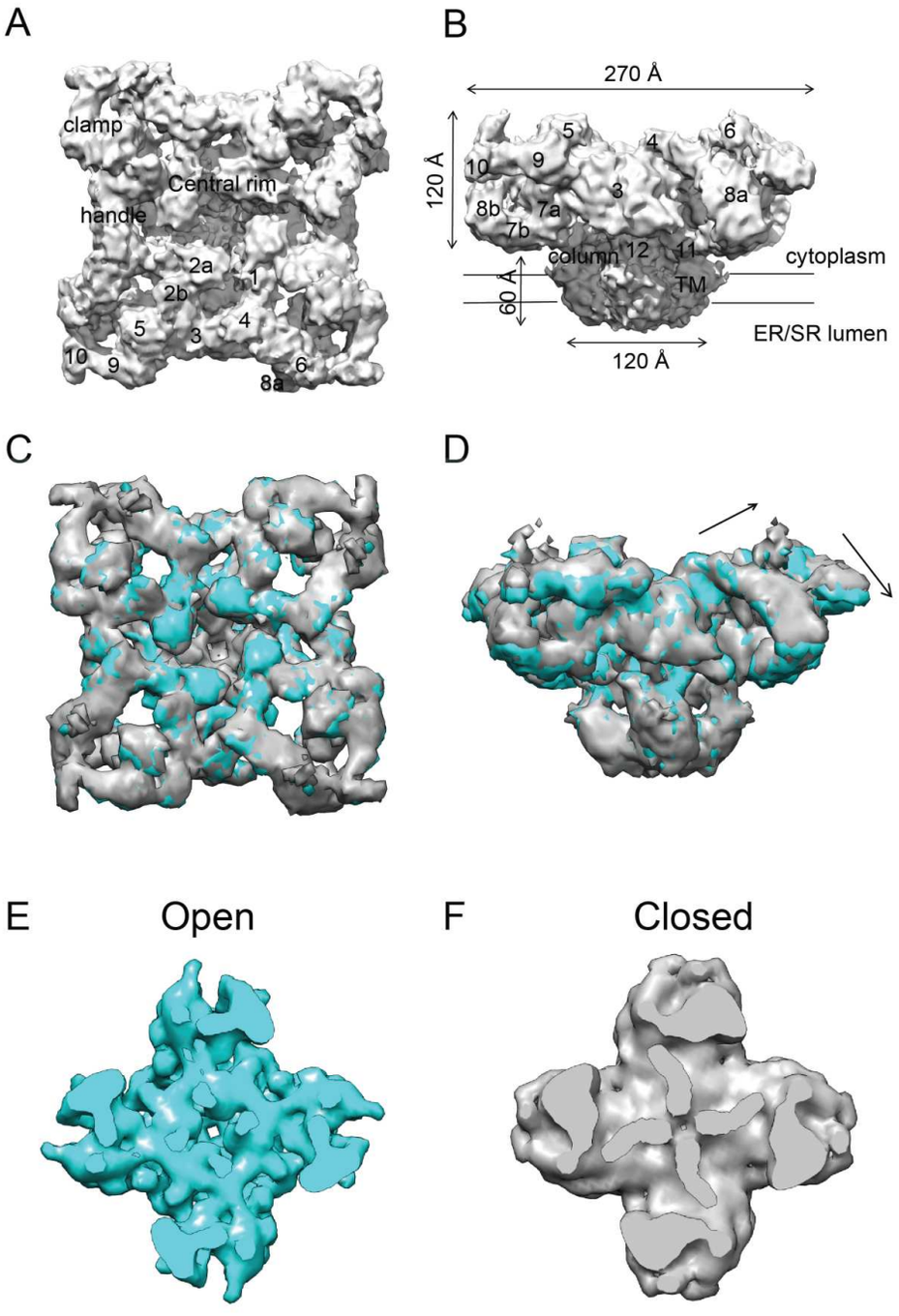

Figure 5. EM maps of RyRs. Top pannels show the top view (A) and side view (B) of the cryo-EM reconstruction of RyR1 in the closed state at 9.6Å (EMDB accession code 1275) [141]. The structural elements and the subregions are labeled. Middle pannels show the top view (C) and side view (D) of the superposition of the RyR1 cryo-EM maps in the closed (gray) and open (cyan) state. (EMDB accession codes 1606 and 1607) [132]. The structural change upon channel opening is indicated by the arrows. Bottom panels show a comparison of the transmembrane region of RyR1 in the open (E) (cyan EMDB accession codes 1606) and closed state (gray EMDB accession codes 1607).

4.2. X-ray crystallographic studies of RyRs

The crystallization of full-length RyRs is a very challenging task due to its large size, membrane protein nature and intrinsic flexibility. Improvement in techniques will likely reveal a high-resolution structure of intact RyRs in the future. The cryo-EM structures have revealed that the RyR is a large modular protein that consists of many small domains. Many efforts have therefore been made to crystallize individual domains or domain clusters that carry important functions.

The first few crystal structures of RyRs that have been solved are of the N-terminal domains (domain A) in RyR1 (residues 1-205) and RyR2 (residues 1-217) [144, 145]. Both display a β-trefoil folding motif (three groups of β-strands that form a triangle structure) that consists of twelve β strands and contains an extra α helix (Figure 6A,B). Domain A spans about one third of the N-terminal disease hot spot. A total of 23 and 9 mutations have been found so far in domain A of RyR1 and RyR2, respectively, many of which cluster in a loop between β strands 8 and 9. Several disease mutants of this domain have been analyzed either by NMR or x-ray crystallography, but none of them showed major structural changes [144, 145] (Figure 7A,B). The observation that most mutations are located on the surface of domain A indicates that they likely affect the interaction of domain A with other domains in RyR or auxiliary proteins.

A severe form of CPVT is caused by the deletion of the entire exon 3 (residues 57-91) from the *ryr2* gene [187, 188]. The structure of wild type domain A shows that exon 3 contributes to a loop region, the 3_{10} helix, β4 strand, and the α helix. One would expect that the complete absence of these structural elements will cause the misfolding of the domain and a loss-of-function phenotype. However, surprisingly, Δexon 3 is not strictly lethal. CPVT symptoms and functional studies suggest a gain-of-function phenotype instead [115]. Even more surprising, the mutant has a higher thermal stability compared to the wild type domain [145]. A crystal structure of RyR2 domain A with Δexon 3 revealed an unusual "structural rescue" scheme: a flexible loop following the exon 3 region replaces the deleted β4 strand and results in a similar overall fold of the domain [147] (Figure 7C). The α helix, however, is lost. The ability to "rescue" a β strand with a random loop segment is highly unusual and suggests that there has been evolutionary pressure to maintain the exact sequence of the flexible loop. Most likely, there is the possibility of alternative splicing, whereby exon 3 is naturally spliced in some cell types. This would represent a mechanism whereby the RyR activity can be fine-tuned in a tissue-specific manner [147]. So far, such a splice variant has not yet been reported.

Up to now, the largest reported crystal structure for all RyRs is for the N-terminal three domains (domain A, B and C, residues 1-559) of RyR1, which covers the majority of the N-terminal disease hot spot [146]. It shows a triangular arrangement of the three domains that interact with each other, mainly through hydrophilic interfaces. Domains A and B have similar β-trefoil folding motifs, while domain C has an armadillo-repeat structure consisting of a bundle of five α-helices (Figure 6C). A total of 76 mutations (RyR1+RyR2) have been identified in these domains. 17 of these are localized at the interfaces between domains A, B and

C (within one subunit). 9 mutations are buried inside the individual domains, and the remaining are on the surface of the ABC structure.

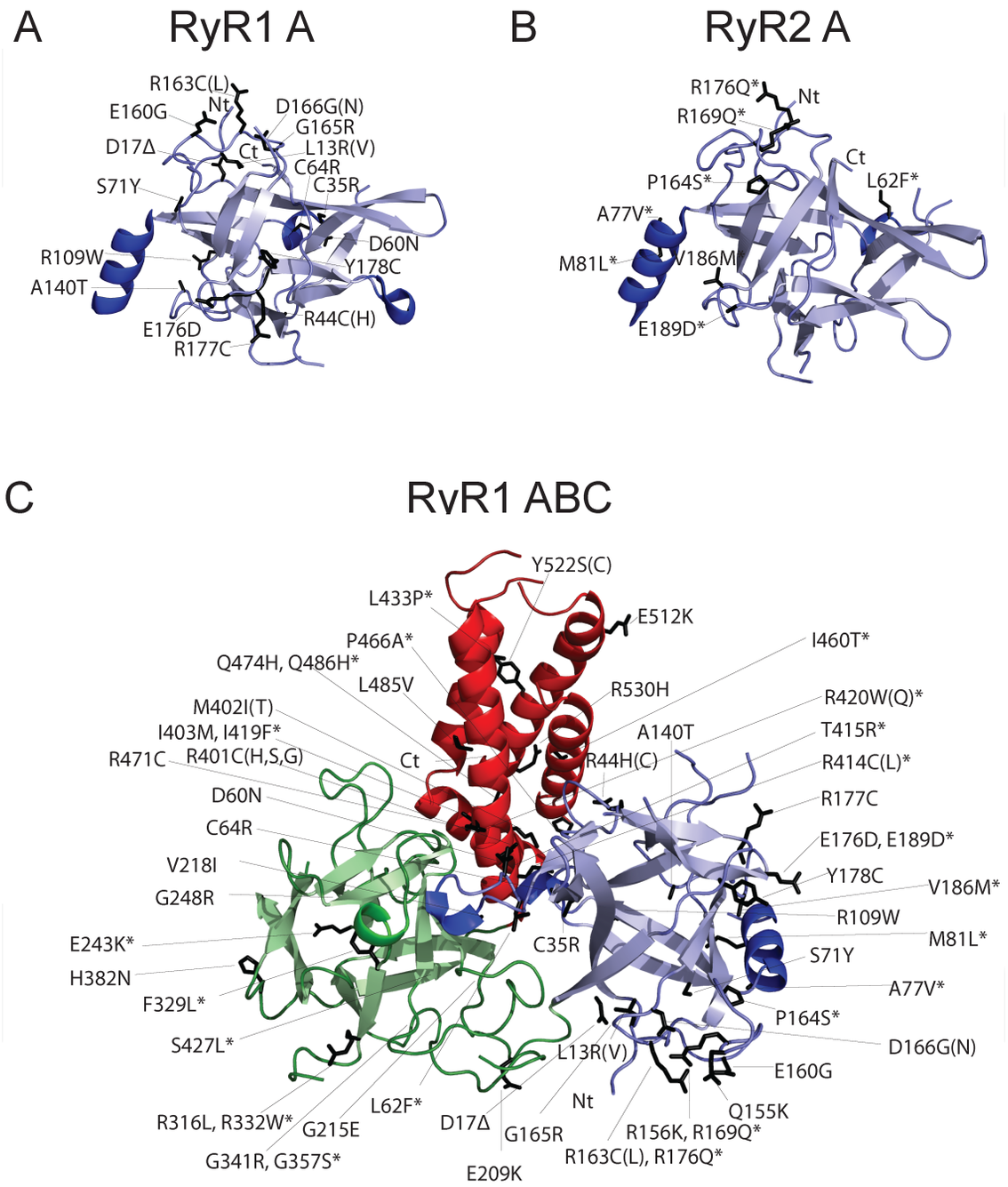

Figure 6. Crystal structures of RyR N-teminal hot spot domains. Shown are crystal structures of (A) RyR1 domain A (pdb: 3ILA), (B) RyR2 domain A (pdb: 3IM5), and (C) RyR1 domain ABC (pdb: 2XOA). α-helices and β-sheets are shown in dark and light colors, respectvely. RyR1 and RyR2 mutations are mapped on the strutural models, indicated by black sticks, and labeled. RyR2 mutations are distinguished from RyR1 mutations by *. Deletion mutations are labeled by Δ. The numbering is according to human RyR1 and RyR2 sequences. The N-terminal and C-terminal positions of the structures are labeled with Nt and Ct, respectively.

Although the EM structure itself usually does not provide the resolution to resolve the atomic positions, the combination of crystal structures and EM structures allows pseudo-atomic models to be built. Individual amino acid residues can thus be located within the overall 3D structure. The high-resolution crystal structures can be docked into the EM maps by matching their electron densities using complex 6 dimensional search algorithms [189-191]. The confidence of the solutions depends on the quality of the EM map, the size of the docked fragments and the agreement of conformations from the two structures. Sometimes a Laplacian filter, which uses an edge-detection algorithm to increase the sensitivity can increase the success rate when a small fragment is used as a search model [191]. Docking of the RyR1 ABC crystal structure into three different cryo-EM maps places it at the same location, the central rim region, forming a cytoplasmic vestibule around the four-fold symmetry axis (Figure 10) [146]. This solution contradicts previous results from insertion experiments which localize the N-terminal hot spot at the clamp region near the corner [167, 168]. The authors suggested that in the GFP-insertion study [168] the long linker and the native flexible loop make it possible for the inserted GFP to be present in a remote location [146]. In addition, the difference density observed in a GST-insertion study splits into two regions, one of which is indeed right beside the central rim region [167]. Interestingly, the location and orientation of domains ABC from the IP_3 receptor, a closely related Ca^{2+}-release channel, are remarkably similar to the docking solution of RyR1 ABC, which further validates the location of the N-terminal region [192].

Locating the N-terminal region within intact RyRs allows several new interfaces to be identified. As the ABC domains dock near the 4-fold symmetry axis, there is a direct interaction between domains A and B from neighboring subunits (Figure 10). In addition, there are five other interfaces between the ABC domains and other regions of RyR1. All the peripheric disease mutations identified in domains ABC are located in one of these six interfaces and none of them are exposed to the surface of the full-length channel, suggesting that they mainly affect the inter-domain interactions rather than interactions between the RyR and other proteins.

The activity of RyRs can be regulated by different types of kinases and phosphotases (Figure 1 and 2). It is believed that the chronic hyperphosphorylation of RyR2 by PKA can dissociate the binding of FKBP12.6 and cause heart failure [193-195], although this result has not been confirmed by other laboratories [118, 196, 197]. Two recent papers reported the structures of a domain containing the phosphorylation sites from all three RyR isoforms [148], and from RyR1 [198] (Figure 8A,B,C). The domain consists of two symmetric halves. Each half contains two α helices, one or more short 3_{10} helices, and a C-terminal β strand. Multiple phosphorylation sites were identified in this domain of RyR2 [148] and most cluster within the same loop. The RyR2 domain doesn't contain any reported disease mutations, but up to 11 disease mutations are found in the RyR1 domain. Interestingly, several disease mutations from this domain are also located close to the phosphorylation sites, suggesting that phosphorylation and disease mutations at this site may have the same effect (Figure 8A). One mutation, L2867G, reduces the melting temperature of the individual domain by 13°C and causes the aggregation of the domain at room temperature (Figure 7D). Several crystal struc-

tures for the other disease mutants were also reported in this study, showing that they affect surface properties and intradomain salt bridges (Figure 7E,F,G) [148]. Docking into the EM map places this domain in the clamp region, but none of the neighbouring domains have been identified thus far (Figure 10). Solving structures of other domains may place more pieces into this big jigsaw and increase our understanding of the isolated domains.

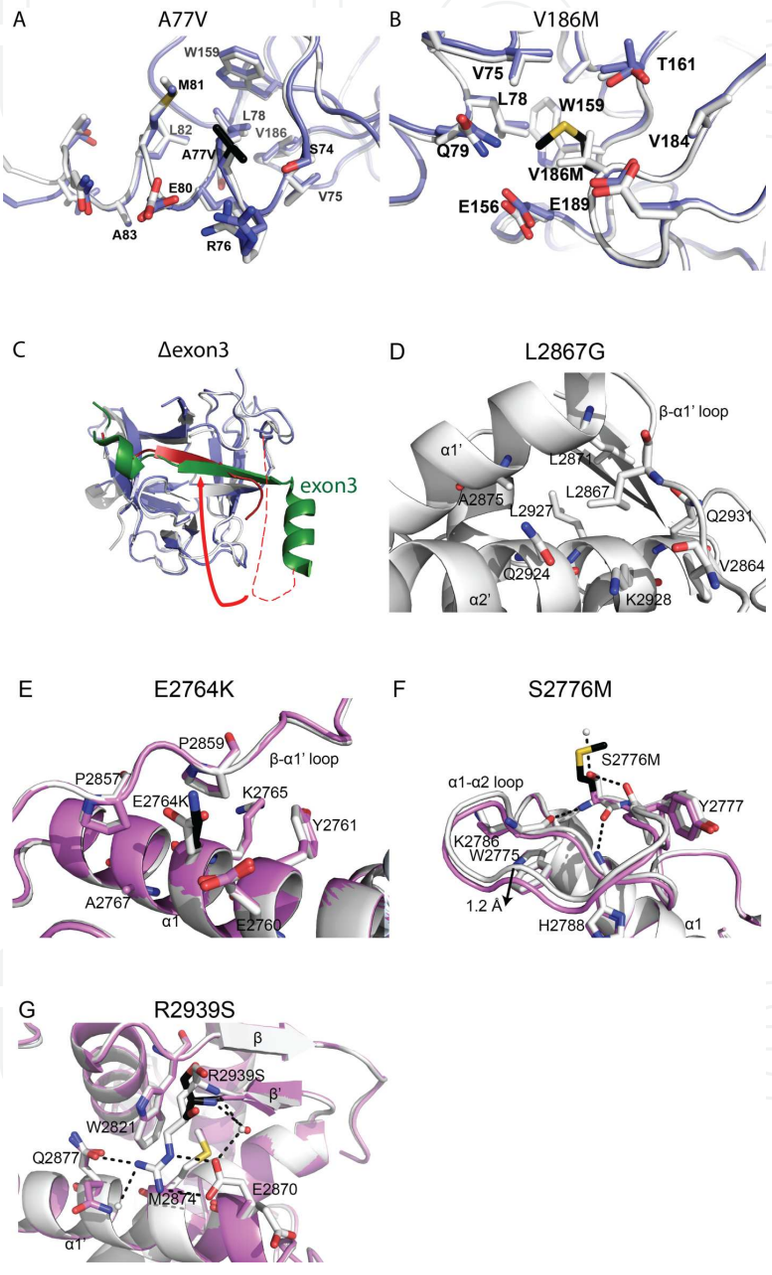

Figure 7. Disease mutant crystal structures. Superposition of the wild-type RyR domains (white) with the mutant structures (colors). Atoms are color coded, with nitrogens in blue, oxygens in red, and sulfurs in yellow. Hydrogen bonds are indicated by dashed lines. All mutants are from RyR1 except the Δexon3 mutant (C) which is from RyR2. (A) A77V, (B) V186M, (C) Δexon3, (D) L2867G mutant (only wild-type structure shown), (E) E2764K, (F) S2776M, (G) R2939S. The single residue mutations are indicated in black. In panel (C), exon 3 is shown in green, and the flexible loop that replaces exon 3 in Δexon3 structure (pdb: 3QR5), is shown in red.

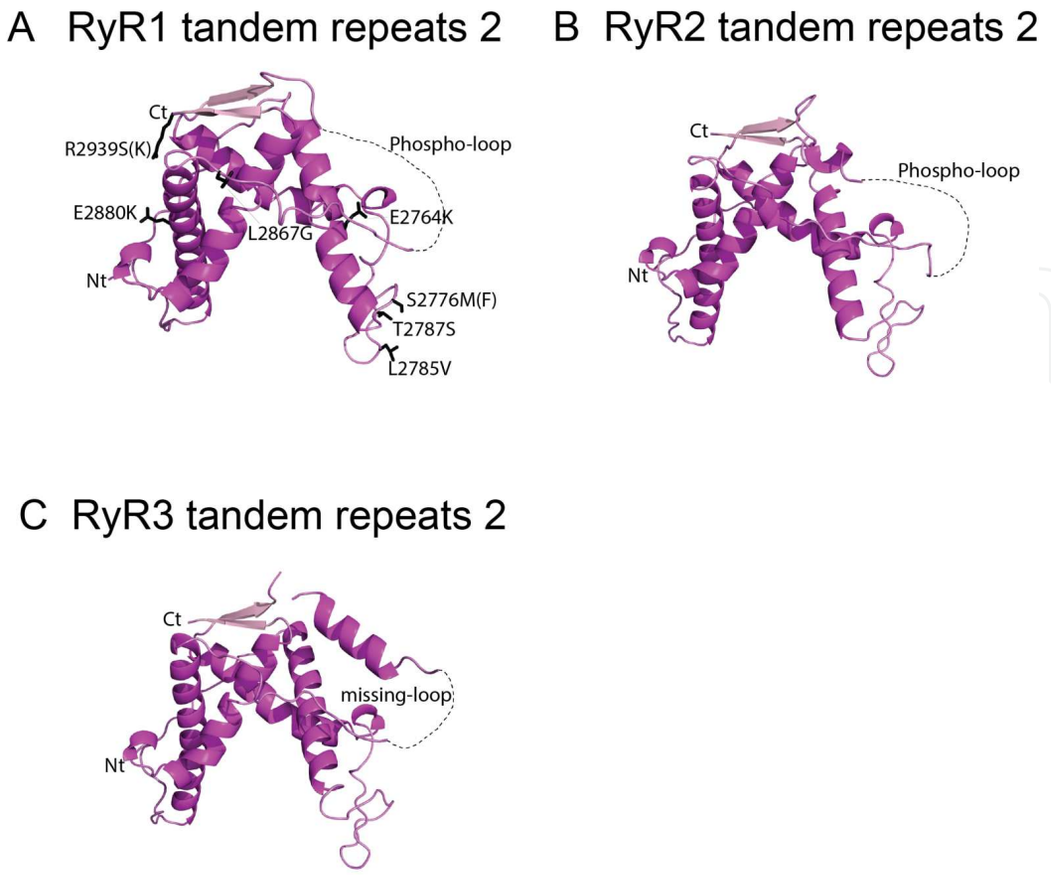

Figure 8. Crystal structures of RyR phosphorylation domains. (A-C) RyR1-3 phosphorylation (tandem repeats 2) domains (pdb: 4ERT, 4ETV, 4ERV, respectively). The phosphorylation loops in RyR1/2 and the corresponding loop in RyR3 are missing in the crystal structures, and indicated by dashed lines in the figures. α-helices and β-sheets are shown in dark and light colors, respectvely. RyR1 mutations are mapped on the strutural models, indicated by black sticks, and labeled. The numbering is according to human RyR1 sequence. The N-terminal and C-terminal positions of the structures are labeled with Nt and Ct, respectively.

4.3. Homology models for RyR domains

So far all the available crystal structures cover ~15% of the full-length RyR in total. There is still a big portion missing. One alternative way to obtain structural informaiton is to create homology models based on known structures using bioinformatics methods. Generally the reliability of a homology model depends on the sequence identities between two proteins, but protein 3D structures tend to be more conserved than their primary sequences during evolution [199]. As the largest ion channel, the evolution of modular RyRs involves the incorporation, loss and duplication of different domains. Protein sequence analysis identifies several domains that are present multiple times in RyR genes, including SPRY domains and tandem repeat domains.

The spore lysis A and RyR (SPRY) domains have been found in many different proteins from bacteria, archaea, viruses and eukaryotes. They are generally known as protein interaction domains [200]. There are three SPRY domains identified in metazoan RyR genes

(SPRY1,2,3) (Figure 3). In skeletal muscle, RyR1 (located in the SR membrane) and $Ca_V1.1$ (located in the plasma membrane) are thought to interact directly. Some biochemical evidence suggest that the RyR1 SPRY2 domain forms an interaction with one of the intracellular loops of $Ca_V1.1$, the so-called II-III loop [201]. Using the phyre2 engine [202], we built homology models for all three SPRY domains of RyR1, based on several known SPRY protein structures (Figure 9A,B,C). All these models show a signature β-sandwich (two stacked β-sheets) folding motif. Interestingly, all ten disease mutations identified in these three SPRYs are located peripherally when mapped into the models (Figure 9A,B,C). As before, it seems that mutations cluster at the surfaces of individual domains, likely affecting interactions with neighboring domains or RyR binding partners. This observation agrees with the known protein interacting properties of the SPRY domain. The mutations in these domains may weaken the interaction with other domains or proteins and change the channel activities.

Another domain fold present in RyRs is the so-called "RyR domain". The latter name is unfortunate, as it obviously is not the only domain present in RyRs. These domains are arranged in tandem repeats, and we will hereafter refer to them as "tandem repeat domains". Each repeat unit is about 100 residues in length, and there are two tandem repeats within each human *ryr* gene: one between SPRY1 and SPRY2, and the other at the central region (Figure 3). These repeat units are also present in bacteria, archaea and viruses, either in single form or in pair with itself or other proteins [203]. The phosphorylation domain mentioned above makes up the second tandem repeat [148]. Interestingly, in a crystal structure of a bacterial repeat domain (pdb code: 3NRT), a single domain dimerizes and presents a similar fold as the paired repeat domain shown in the phosphorylation domain structure. We created a homology model for the first tandem repeats from RyR1 based on these two protein structures [202]. (Figure 9D). Seven mutations are found on this tandem repeat. Five of these are located on the surface, likely affecting interactions with other domains or RyR binding partners. The remaining two are buried within the domain, and may thus affect the overall folding stability.

Although the total number of the TM helices in RyRs is not clear, from the secondary structure prediction, their last two TM helices clearly share homology with the pore-forming regions of potassium channels and bacterial voltage-gated sodium channels (Na_V). Because the pore-forming region is directly responsible for passage of Ca^{2+} ions through the SR membrane, any minor structural alteration in this region may directly interfere with the ion conduction. Indeed, up to 50 mutations (RyR1+RyR2) have been identified in this region, which consists of only 125 residues. The occurrence of one mutation per 2.5 residues makes the pore-forming region into a "super-hot" disease hot spot. We created a model for the RyR1 pore-forming domain based on several bacterial NaV structures (Figure 9E). Most mutations cluster in the top half (ER luminal side) of the domain. Interestingly, 31 out of 41 RyR1 mutations in this domain are associated with CCD, which can be caused by the loss-of-function of RyRs. Therefore, it seems that many mutations in the TM domain can directly block the ion conduction pathway and reduce channel activity, while mutations in the cytoplasmic domains tend to destabilize the closed state of the channel and make it "leaky".

http://dx.doi.org/10.5772/53641

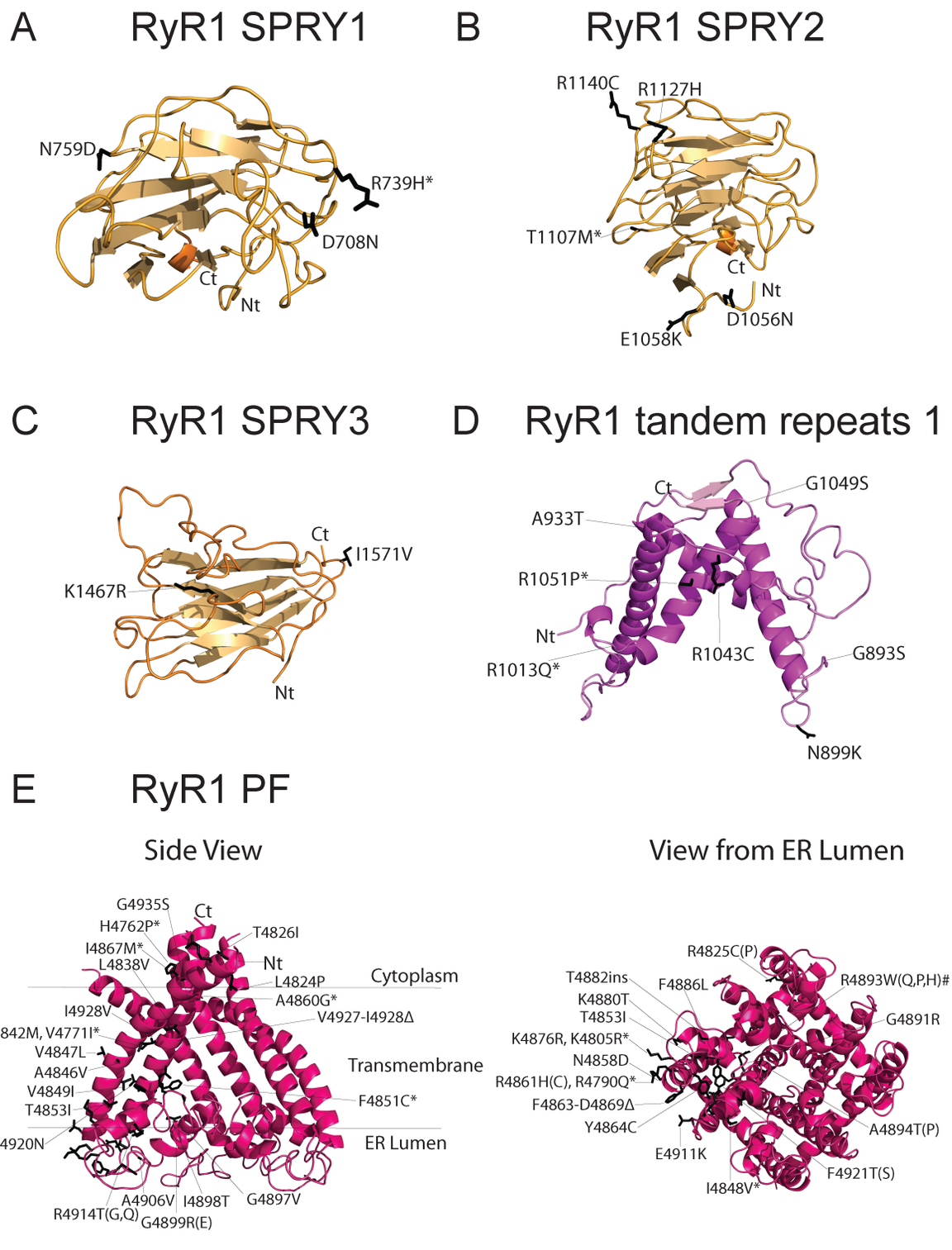

Figure 9. Homology structural models of RyR domains. Structural models were created by Phyre2 server [202]: (A-C) RyR1 SPRY 1-3, (D) RyR1 repeats 1, and (E) RyR1 pore-forming domain (PF). α-helices and β-sheets are shown in dark and light color, respectvely. RyR1 and RyR2 mutations are mapped on the strutural models, indicated by black sticks, and labeled. RyR2 mutations are distinguished from RyR1 mutations by *. Deletion mutations are labeled by Δ and insertion mutations are labeled by ins. The numbering is according to human RyR1 and RyR2 sequences. The N-terminal and C-terminal positions of the structures are labeled with Nt and Ct, respectively.

Like the previous studies with crystal structures, knowing the exact locations of these domains in the full length channel will deepen our understanding of the channel in the normal and disease states. But technically it is dangerous to dock homology models into the EM maps due to their limited accuracy. However, these models can still provide a good template to guide the design of the insertion sites for the EM studies, which will help to reveal the location of these domains and the corresponding disease mutations.

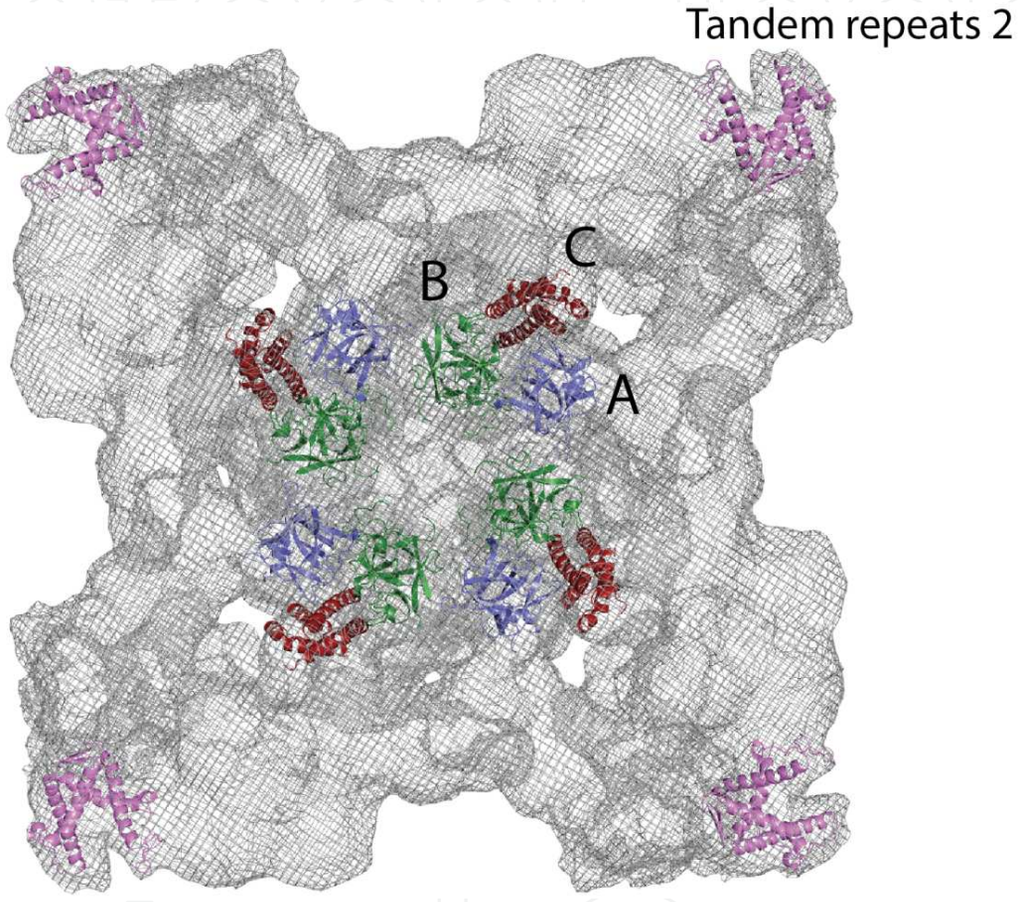

Figure 10. Pseudo-atomic models. Top view of the 9.6 Å RyR1 cryo-EM map (EMDB accession code 1275), showing the docked positions of the N-terminal disease hot spot (domain A (blue), B(green), C(red)) and the phosphorylation domain (purple) [141].

5. Conclusion

The available crystal structures and homology models represent ~32% of the full length RyRs. In the years to come, further crystallographic studies on predicted domains, and their localization into full-length RyRs will likely shed more light. Although obtaining well-diffracting crystals of intact RyRs may be an arduous task, this will ultimately be necessary to fully understand the function of RyRs in health and disease.

Author details

Zhiguang Yuchi, Lynn Kimlicka and Filip Van Petegem*

*Address all correspondence to: filip.vanpetegem@gmail.com

Department of Biochemistry and Molecular Biology, University of British Columbia, Vancouver, British Columbia, Canada

References

[1] Endo, M., M. Tanaka, and Y. Ogawa, Calcium induced release of calcium from the sarcoplasmic reticulum of skinned skeletal muscle fibres. Nature, 1970. 228(5266): p. 34-6.

[2] Fabiato, A., Calcium-induced release of calcium from the cardiac sarcoplasmic reticulum. The American journal of physiology, 1983. 245(1): p. C1-14.

[3] Block, B.A., et al., Structural evidence for direct interaction between the molecular components of the transverse tubule/sarcoplasmic reticulum junction in skeletal muscle. J Cell Biol, 1988. 107(6 Pt 2): p. 2587-600.

[4] Tanabe, T., et al., Regions of the skeletal muscle dihydropyridine receptor critical for excitation-contraction coupling. Nature, 1990. 346(6284): p. 567-9.

[5] Tanabe, T., et al., Restoration of excitation-contraction coupling and slow calcium current in dysgenic muscle by dihydropyridine receptor complementary DNA. Nature, 1988. 336(6195): p. 134-9.

[6] Rios, E. and G. Brum, Involvement of dihydropyridine receptors in excitation-contraction coupling in skeletal muscle. Nature, 1987. 325(6106): p. 717-20.

[7] Rogers, E.F., F.R. Koniuszy, and et al., Plant insecticides; ryanodine, a new alkaloid from Ryania speciosa Vahl. J Am Chem Soc, 1948. 70(9): p. 3086-8.

[8] Lai, F.A., et al., Purification and reconstitution of the calcium release channel from skeletal muscle. Nature, 1988. 331(6154): p. 315-9.

[9] Inui, M., A. Saito, and S. Fleischer, Purification of the ryanodine receptor and identity with feet structures of junctional terminal cisternae of sarcoplasmic reticulum from fast skeletal muscle. J Biol Chem, 1987. 262(4): p. 1740-7.

[10] Takeshima, H., et al., Primary structure and expression from complementary DNA of skeletal muscle ryanodine receptor. Nature, 1989. 339(6224): p. 439-45.

[11] Zorzato, F., et al., Molecular cloning of cDNA encoding human and rabbit forms of the Ca2+ release channel (ryanodine receptor) of skeletal muscle sarcoplasmic reticulum. J Biol Chem, 1990. 265(4): p. 2244-56.

[12] Otsu, K., et al., Molecular cloning of cDNA encoding the Ca2+ release channel (ryanodine receptor) of rabbit cardiac muscle sarcoplasmic reticulum. J Biol Chem, 1990. 265(23): p. 13472-83.

[13] Nakai, J., et al., Primary structure and functional expression from cDNA of the cardiac ryanodine receptor/calcium release channel. FEBS Lett, 1990. 271(1-2): p. 169-77.

[14] Hakamata, Y., et al., Primary structure and distribution of a novel ryanodine receptor/calcium release channel from rabbit brain. FEBS Lett, 1992. 312(2-3): p. 229-35.

[15] Lanner, J.T., et al., Ryanodine receptors: structure, expression, molecular details, and function in calcium release. Cold Spring Harb Perspect Biol, 2010. 2(11): p. a003996.

[16] Zalk, R., S.E. Lehnart, and A.R. Marks, Modulation of the ryanodine receptor and intracellular calcium. Annu Rev Biochem, 2007. 76: p. 367-85.

[17] Van Petegem, F., Ryanodine Receptors: Structure and Function. The Journal of biological chemistry, 2012.

[18] Palade, P., R.D. Mitchell, and S. Fleischer, Spontaneous calcium release from sarcoplasmic reticulum. General description and effects of calcium. J Biol Chem, 1983. 258(13): p. 8098-107.

[19] Jiang, D., et al., RyR2 mutations linked to ventricular tachycardia and sudden death reduce the threshold for store-overload-induced Ca2+ release (SOICR). Proc Natl Acad Sci U S A, 2004. 101(35): p. 13062-7.

[20] Ahern, G.P., P.R. Junankar, and A.F. Dulhunty, Subconductance states in single-channel activity of skeletal muscle ryanodine receptors after removal of FKBP12. Biophys J, 1997. 72(1): p. 146-62.

[21] Chelu, M.G., et al., Regulation of ryanodine receptors by FK506 binding proteins. Trends Cardiovasc Med, 2004. 14(6): p. 227-34.

[22] Ikemoto, T., M. Iino, and M. Endo, Enhancing effect of calmodulin on Ca(2+)-induced Ca2+ release in the sarcoplasmic reticulum of rabbit skeletal muscle fibres. J Physiol, 1995. 487 (Pt 3): p. 573-82.

[23] Tripathy, A., et al., Calmodulin activation and inhibition of skeletal muscle Ca2+ release channel (ryanodine receptor). Biophys J, 1995. 69(1): p. 106-19.

[24] Buratti, R., et al., Calcium dependent activation of skeletal muscle Ca2+ release channel (ryanodine receptor) by calmodulin. Biochem Biophys Res Commun, 1995. 213(3): p. 1082-90.

[25] Fuentes, O., et al., Calcium-dependent block of ryanodine receptor channel of swine skeletal muscle by direct binding of calmodulin. Cell calcium, 1994. 15(4): p. 305-16.

[26] Zalk, R., S.E. Lehnart, and A.R. Marks, Modulation of the Ryanodine Receptor and Intracellular Calcium. Annual Review of Biochemistry, 2007. 76(1): p. 367-385.

[27] Monnier, N., et al., Malignant-hyperthermia susceptibility is associated with a mutation of the alpha 1-subunit of the human dihydropyridine-sensitive L-type voltage-dependent calcium-channel receptor in skeletal muscle. Am J Hum Genet, 1997. 60(6): p. 1316-25.

[28] Rosenberg, H., et al., Malignant hyperthermia. Orphanet journal of rare diseases, 2007. 2: p. 21.

[29] Maclennan, D.H. and E. Zvaritch, Mechanistic models for muscle diseases and disorders originating in the sarcoplasmic reticulum. Biochim Biophys Acta, 2011. 1813(5): p. 948-64.

[30] Krause, T., et al., Dantrolene--a review of its pharmacology, therapeutic use and new developments. Anaesthesia, 2004. 59(4): p. 364-73.

[31] Paul-Pletzer, K., et al., Identification of a dantrolene-binding sequence on the skeletal muscle ryanodine receptor. J Biol Chem, 2002. 277(38): p. 34918-23.

[32] Zhao, F., et al., Dantrolene inhibition of ryanodine receptor Ca2+ release channels. Molecular mechanism and isoform selectivity. J Biol Chem, 2001. 276(17): p. 13810-6.

[33] Fujii, J., et al., Identification of a mutation in porcine ryanodine receptor associated with malignant hyperthermia. Science, 1991. 253(5018): p. 448-51.

[34] Gillard, E.F., et al., A substitution of cysteine for arginine 614 in the ryanodine receptor is potentially causative of human malignant hyperthermia. Genomics, 1991. 11(3): p. 751-5.

[35] Klingler, W., et al., Core myopathies and risk of malignant hyperthermia. Anesth Analg, 2009. 109(4): p. 1167-73.

[36] Robinson, R., et al., Mutations in RYR1 in malignant hyperthermia and central core disease. Hum Mutat, 2006. 27(10): p. 977-89.

[37] Denborough, M.A., X. Dennett, and R.M. Anderson, Central-core disease and malignant hyperpyrexia. British medical journal, 1973. 1(5848): p. 272-3.

[38] Jungbluth, H., et al., Minicore myopathy with ophthalmoplegia caused by mutations in the ryanodine receptor type 1 gene. Neurology, 2005. 65(12): p. 1930-5.

[39] Ferreiro, A., et al., Mutations of the selenoprotein N gene, which is implicated in rigid spine muscular dystrophy, cause the classical phenotype of multiminicore disease: reassessing the nosology of early-onset myopathies. Am J Hum Genet, 2002. 71(4): p. 739-49.

[40] Jurynec, M.J., et al., Selenoprotein N is required for ryanodine receptor calcium release channel activity in human and zebrafish muscle. Proc Natl Acad Sci U S A, 2008. 105(34): p. 12485-90.

[41] Kaindl, A.M., et al., Missense mutations of ACTA1 cause dominant congenital myopathy with cores. J Med Genet, 2004. 41(11): p. 842-8.

[42] Priori, S.G., et al., Mutations in the cardiac ryanodine receptor gene (hRyR2) underlie catecholaminergic polymorphic ventricular tachycardia. Circulation, 2001. 103(2): p. 196-200.

[43] Lahat, H., et al., A missense mutation in a highly conserved region of CASQ2 is associated with autosomal recessive catecholamine-induced polymorphic ventricular tachycardia in Bedouin families from Israel. American journal of human genetics, 2001. 69(6): p. 1378-84.

[44] Roux-Buisson, N., et al., Absence of triadin, a protein of the calcium release complex, is responsible for cardiac arrhythmia with sudden death in human. Human molecular genetics, 2012. 21(12): p. 2759-67.

[45] Pflaumer, A. and A.M. Davis, Guidelines for the diagnosis and management of Catecholaminergic Polymorphic Ventricular Tachycardia. Heart, lung & circulation, 2012. 21(2): p. 96-100.

[46] Watanabe, H., et al., Flecainide prevents catecholaminergic polymorphic ventricular tachycardia in mice and humans. Nat Med, 2009. 15(4): p. 380-3.

[47] Ohnishi, S.T., S. Taylor, and G.A. Gronert, Calcium-induced Ca2+ release from sarcoplasmic reticulum of pigs susceptible to malignant hyperthermia. The effects of halothane and dantrolene. FEBS Lett, 1983. 161(1): p. 103-7.

[48] Ohnishi, S.T., Effects of halothane, caffeine, dantrolene and tetracaine on the calcium permeability of skeletal sarcoplasmic reticulum of malignant hyperthermic pigs. Biochim Biophys Acta, 1987. 897(2): p. 261-8.

[49] Nelson, T.E., Abnormality in calcium release from skeletal sarcoplasmic reticulum of pigs susceptible to malignant hyperthermia. J Clin Invest, 1983. 72(3): p. 862-70.

[50] Mickelson, J.R., et al., Abnormal sarcoplasmic reticulum ryanodine receptor in malignant hyperthermia. J Biol Chem, 1988. 263(19): p. 9310-5.

[51] Mickelson, J.R., et al., Stimulation and inhibition of [3H]ryanodine binding to sarcoplasmic reticulum from malignant hyperthermia susceptible pigs. Arch Biochem Biophys, 1990. 278(1): p. 251-7.

[52] Fill, M., et al., Abnormal ryanodine receptor channels in malignant hyperthermia. Biophys J, 1990. 57(3): p. 471-5.

[53] Nelson, T.E., Halothane effects on human malignant hyperthermia skeletal muscle single calcium-release channels in planar lipid bilayers. Anesthesiology, 1992. 76(4): p. 588-95.

[54] Shomer, N.H., et al., Reconstitution of abnormalities in the malignant hyperthermia-susceptible pig ryanodine receptor. Am J Physiol, 1993. 264(1 Pt 1): p. C125-35.

[55] Richter, M., et al., Functional characterization of a distinct ryanodine receptor mutation in human malignant hyperthermia-susceptible muscle. J Biol Chem, 1997. 272(8): p. 5256-60.

[56] Wehner, M., et al., Increased sensitivity to 4-chloro-m-cresol and caffeine in primary myotubes from malignant hyperthermia susceptible individuals carrying the ryanodine receptor 1 Thr2206Met (C6617T) mutation. Clin Genet, 2002. 62(2): p. 135-46.

[57] Wehner, M., et al., The Ile2453Thr mutation in the ryanodine receptor gene 1 is associated with facilitated calcium release from sarcoplasmic reticulum by 4-chloro-m-cresol in human myotubes. Cell Calcium, 2003. 34(2): p. 163-8.

[58] Wehner, M., et al., Functional characterization of malignant hyperthermia-associated RyR1 mutations in exon 44, using the human myotube model. Neuromuscul Disord, 2004. 14(7): p. 429-37.

[59] Kaufmann, A., et al., Novel double and single ryanodine receptor 1 variants in two Austrian malignant hyperthermia families. Anesth Analg, 2012. 114(5): p. 1017-25.

[60] Chelu, M.G., et al., Heat- and anesthesia-induced malignant hyperthermia in an RyR1 knock-in mouse. FASEB J, 2006. 20(2): p. 329-30.

[61] Yang, T., et al., Pharmacologic and functional characterization of malignant hyperthermia in the R163C RyR1 knock-in mouse. Anesthesiology, 2006. 105(6): p. 1164-75.

[62] Zvaritch, E., et al., An Ryr1I4895T mutation abolishes Ca2+ release channel function and delays development in homozygous offspring of a mutant mouse line. Proc Natl Acad Sci U S A, 2007. 104(47): p. 18537-42.

[63] Durham, W.J., et al., RyR1 S-nitrosylation underlies environmental heat stroke and sudden death in Y522S RyR1 knockin mice. Cell, 2008. 133(1): p. 53-65.

[64] Andronache, Z., et al., A retrograde signal from RyR1 alters DHP receptor inactivation and limits window Ca2+ release in muscle fibers of Y522S RyR1 knock-in mice. Proc Natl Acad Sci U S A, 2009. 106(11): p. 4531-6.

[65] Bannister, R.A., et al., A malignant hyperthermia-inducing mutation in RYR1 (R163C): consequent alterations in the functional properties of DHPR channels. J Gen Physiol, 2010. 135(6): p. 629-40.

[66] Esteve, E., et al., A malignant hyperthermia-inducing mutation in RYR1 (R163C): alterations in Ca2+ entry, release, and retrograde signaling to the DHPR. J Gen Physiol, 2010. 135(6): p. 619-28.

[67] Feng, W., et al., Functional and biochemical properties of ryanodine receptor type 1 channels from heterozygous R163C malignant hyperthermia-susceptible mice. Mol Pharmacol, 2011. 79(3): p. 420-31.

[68] Liu, N., et al., Arrhythmogenesis in catecholaminergic polymorphic ventricular tachycardia: insights from a RyR2 R4496C knock-in mouse model. Circ Res, 2006. 99(3): p. 292-8.

[69] Lehnart, S.E., et al., Leaky Ca2+ release channel/ryanodine receptor 2 causes seizures and sudden cardiac death in mice. J Clin Invest, 2008. 118(6): p. 2230-45.

[70] Goddard, C.A., et al., Physiological consequences of the P2328S mutation in the ryanodine receptor (RyR2) gene in genetically modified murine hearts. Acta Physiol (Oxf), 2008. 194(2): p. 123-40.

[71] Fernandez-Velasco, M., et al., Increased Ca2+ sensitivity of the ryanodine receptor mutant RyR2R4496C underlies catecholaminergic polymorphic ventricular tachycardia. Circ Res, 2009. 104(2): p. 201-9, 12p following 209.

[72] Kashimura, T., et al., In the RyR2(R4496C) mouse model of CPVT, beta-adrenergic stimulation induces Ca waves by increasing SR Ca content and not by decreasing the threshold for Ca waves. Circ Res, 2010. 107(12): p. 1483-9.

[73] Suetomi, T., et al., Mutation-linked defective interdomain interactions within ryanodine receptor cause aberrant Ca(2)(+)release leading to catecholaminergic polymorphic ventricular tachycardia. Circulation, 2011. 124(6): p. 682-94.

[74] Boncompagni, S., et al., The I4895T mutation in the type 1 ryanodine receptor induces fiber-type specific alterations in skeletal muscle that mimic premature aging. Aging Cell, 2010. 9(6): p. 958-70.

[75] Loy, R.E., et al., Muscle weakness in Ryr1I4895T/WT knock-in mice as a result of reduced ryanodine receptor Ca2+ ion permeation and release from the sarcoplasmic reticulum. J Gen Physiol, 2011. 137(1): p. 43-57.

[76] Barrientos, G.C., et al., Gene dose influences cellular and calcium channel dysregulation in heterozygous and homozygous T4826I-RYR1 malignant hyperthermia-susceptible muscle. J Biol Chem, 2012. 287(4): p. 2863-76.

[77] Ghassemi, F., et al., A recessive ryanodine receptor 1 mutation in a CCD patient increases channel activity. Cell Calcium, 2009. 45(2): p. 192-7.

[78] Tilgen, N., et al., Identification of four novel mutations in the C-terminal membrane spanning domain of the ryanodine receptor 1: association with central core disease and alteration of calcium homeostasis. Hum Mol Genet, 2001. 10(25): p. 2879-87.

[79] Zorzato, F., et al., Clinical and functional effects of a deletion in a COOH-terminal lumenal loop of the skeletal muscle ryanodine receptor. Hum Mol Genet, 2003. 12(4): p. 379-88.

[80] Lyfenko, A.D., et al., Two central core disease (CCD) deletions in the C-terminal region of RYR1 alter muscle excitation-contraction (EC) coupling by distinct mechanisms. Hum Mutat, 2007. 28(1): p. 61-8.

[81] Anderson, A.A., et al., Identification and biochemical characterization of a novel ryanodine receptor gene mutation associated with malignant hyperthermia. Anesthesiology, 2008. 108(2): p. 208-15.

[82] Zullo, A., et al., Functional characterization of ryanodine receptor (RYR1) sequence variants using a metabolic assay in immortalized B-lymphocytes. Hum Mutat, 2009. 30(4): p. E575-90.

[83] Vukcevic, M., et al., Functional properties of RYR1 mutations identified in Swedish patients with malignant hyperthermia and central core disease. Anesth Analg, 2010. 111(1): p. 185-90.

[84] Avila, G., J.J. O'Brien, and R.T. Dirksen, Excitation--contraction uncoupling by a human central core disease mutation in the ryanodine receptor. Proc Natl Acad Sci U S A, 2001. 98(7): p. 4215-20.

[85] Avila, G. and R.T. Dirksen, Functional effects of central core disease mutations in the cytoplasmic region of the skeletal muscle ryanodine receptor. J Gen Physiol, 2001. 118(3): p. 277-90.

[86] Yang, T., et al., Functional defects in six ryanodine receptor isoform-1 (RyR1) mutations associated with malignant hyperthermia and their impact on skeletal excitation-contraction coupling. J Biol Chem, 2003. 278(28): p. 25722-30.

[87] Avila, G., K.M. O'Connell, and R.T. Dirksen, The pore region of the skeletal muscle ryanodine receptor is a primary locus for excitation-contraction uncoupling in central core disease. J Gen Physiol, 2003. 121(4): p. 277-86.

[88] Dirksen, R.T. and G. Avila, Distinct effects on Ca2+ handling caused by malignant hyperthermia and central core disease mutations in RyR1. Biophys J, 2004. 87(5): p. 3193-204.

[89] Brini, M., et al., Ca2+ signaling in HEK-293 and skeletal muscle cells expressing recombinant ryanodine receptors harboring malignant hyperthermia and central core disease mutations. J Biol Chem, 2005. 280(15): p. 15380-9.

[90] Zhou, H., et al., Multi-minicore disease and atypical periodic paralysis associated with novel mutations in the skeletal muscle ryanodine receptor (RYR1) gene. Neuromuscul Disord, 2010. 20(3): p. 166-73.

[91] Tong, J., et al., Caffeine and halothane sensitivity of intracellular Ca2+ release is altered by 15 calcium release channel (ryanodine receptor) mutations associated with malignant hyperthermia and/or central core disease. J Biol Chem, 1997. 272(42): p. 26332-9.

[92] Du, G.G. and D.H. MacLennan, Functional consequences of mutations of conserved, polar amino acids in transmembrane sequences of the Ca2+ release channel (ryanodine receptor) of rabbit skeletal muscle sarcoplasmic reticulum. J Biol Chem, 1998. 273(48): p. 31867-72.

[93] Lynch, P.J., et al., A mutation in the transmembrane/luminal domain of the ryanodine receptor is associated with abnormal Ca2+ release channel function and severe central core disease. Proc Natl Acad Sci U S A, 1999. 96(7): p. 4164-9.

[94] Tong, J., T.V. McCarthy, and D.H. MacLennan, Measurement of resting cytosolic Ca2+ concentrations and Ca2+ store size in HEK-293 cells transfected with malignant hyperthermia or central core disease mutant Ca2+ release channels. J Biol Chem, 1999. 274(2): p. 693-702.

[95] Du, G.G., et al., Mutations to Gly2370, Gly2373 or Gly2375 in malignant hyperthermia domain 2 decrease caffeine and cresol sensitivity of the rabbit skeletal-muscle Ca2+-release channel (ryanodine receptor isoform 1). Biochem J, 2001. 360(Pt 1): p. 97-105.

[96] Sambuughin, N., et al., Identification and functional characterization of a novel ryanodine receptor mutation causing malignant hyperthermia in North American and South American families. Neuromuscul Disord, 2001. 11(6-7): p. 530-7.

[97] Loke, J.C., et al., Detection of a novel ryanodine receptor subtype 1 mutation (R328W) in a malignant hyperthermia family by sequencing of a leukocyte transcript. Anesthesiology, 2003. 99(2): p. 297-302.

[98] Du, G.G., et al., Central core disease mutations R4892W, I4897T and G4898E in the ryanodine receptor isoform 1 reduce the Ca2+ sensitivity and amplitude of Ca2+-dependent Ca2+ release. Biochem J, 2004. 382(Pt 2): p. 557-64.

[99] Zhou, H., et al., Characterization of recessive RYR1 mutations in core myopathies. Hum Mol Genet, 2006. 15(18): p. 2791-803.

[100] Xu, L., et al., Single channel properties of heterotetrameric mutant RyR1 ion channels linked to core myopathies. J Biol Chem, 2008. 283(10): p. 6321-9.

[101] Jiang, D., et al., Reduced threshold for luminal Ca2+ activation of RyR1 underlies a causal mechanism of porcine malignant hyperthermia. J Biol Chem, 2008. 283(30): p. 20813-20.

[102] Migita, T., et al., Functional analysis of ryanodine receptor type 1 p.R2508C mutation in exon 47. J Anesth, 2009. 23(3): p. 341-6.

[103] Sato, K., N. Pollock, and K.M. Stowell, Functional studies of RYR1 mutations in the skeletal muscle ryanodine receptor using human RYR1 complementary DNA. Anesthesiology, 2010. 112(6): p. 1350-4.

[104] Haraki, T., et al., Mutated p.4894 RyR1 function related to malignant hyperthermia and congenital neuromuscular disease with uniform type 1 fiber (CNMDU1). Anesth Analg, 2011. 113(6): p. 1461-7.

[105] Jiang, D., et al., Enhanced basal activity of a cardiac Ca2+ release channel (ryanodine receptor) mutant associated with ventricular tachycardia and sudden death. Circ Res, 2002. 91(3): p. 218-25.

[106] Thomas, N.L., C.H. George, and F.A. Lai, Functional heterogeneity of ryanodine receptor mutations associated with sudden cardiac death. Cardiovasc Res, 2004. 64(1): p. 52-60.

[107] Lehnart, S.E., et al., Sudden death in familial polymorphic ventricular tachycardia associated with calcium release channel (ryanodine receptor) leak. Circulation, 2004. 109(25): p. 3208-14.

[108] Jiang, D., et al., Enhanced store overload-induced Ca2+ release and channel sensitivity to luminal Ca2+ activation are common defects of RyR2 mutations linked to ventricular tachycardia and sudden death. Circ Res, 2005. 97(11): p. 1173-81.

[109] Thomas, N.L., F.A. Lai, and C.H. George, Differential Ca2+ sensitivity of RyR2 mutations reveals distinct mechanisms of channel dysfunction in sudden cardiac death. Biochem Biophys Res Commun, 2005. 331(1): p. 231-8.

[110] Jiang, D., et al., Loss of luminal Ca2+ activation in the cardiac ryanodine receptor is associated with ventricular fibrillation and sudden death. Proc Natl Acad Sci U S A, 2007. 104(46): p. 18309-14.

[111] Tester, D.J., et al., A mechanism for sudden infant death syndrome (SIDS): stress-induced leak via ryanodine receptors. Heart Rhythm, 2007. 4(6): p. 733-9.

[112] Jones, P.P., et al., Endoplasmic reticulum Ca2+ measurements reveal that the cardiac ryanodine receptor mutations linked to cardiac arrhythmia and sudden death alter the threshold for store-overload-induced Ca2+ release. Biochem J, 2008. 412(1): p. 171-8.

[113] Jiang, D., et al., Characterization of a novel mutation in the cardiac ryanodine receptor that results in catecholaminergic polymorphic ventricular tachycardia. Channels (Austin), 2010. 4(4): p. 302-10.

[114] Meli, A.C., et al., A novel ryanodine receptor mutation linked to sudden death increases sensitivity to cytosolic calcium. Circ Res, 2011. 109(3): p. 281-90.

[115] Tang, Y., et al., Abnormal termination of Ca2+ release is a common defect of RyR2 mutations associated with cardiomyopathies. Circ Res, 2012. 110(7): p. 968-77.

[116] Treves, S., et al., Alteration of intracellular Ca2+ transients in COS-7 cells transfected with the cDNA encoding skeletal-muscle ryanodine receptor carrying a mutation associated with malignant hyperthermia. Biochem J, 1994. 301 (Pt 3): p. 661-5.

[117] Otsu, K., et al., The point mutation Arg615-->Cys in the Ca2+ release channel of skeletal sarcoplasmic reticulum is responsible for hypersensitivity to caffeine and halothane in malignant hyperthermia. J Biol Chem, 1994. 269(13): p. 9413-5.

[118] George, C.H., G.V. Higgs, and F.A. Lai, Ryanodine receptor mutations associated with stress-induced ventricular tachycardia mediate increased calcium release in stimulated cardiomyocytes. Circ Res, 2003. 93(6): p. 531-40.

[119] George, C.H., et al., Arrhythmogenic mutation-linked defects in ryanodine receptor autoregulation reveal a novel mechanism of Ca2+ release channel dysfunction. Circ Res, 2006. 98(1): p. 88-97.

[120] Boncompagni, S., et al., Characterization and temporal development of cores in a mouse model of malignant hyperthermia. Proc Natl Acad Sci U S A, 2009. 106(51): p. 21996-2001.

[121] Zvaritch, E., et al., Ca2+ dysregulation in Ryr1(I4895T/wt) mice causes congenital myopathy with progressive formation of minicores, cores, and nemaline rods. Proc Natl Acad Sci U S A, 2009. 106(51): p. 21813-8.

[122] Yuen, B., et al., Mice expressing T4826I-RYR1 are viable but exhibit sex- and genotype-dependent susceptibility to malignant hyperthermia and muscle damage. FASEB J, 2012. 26(3): p. 1311-22.

[123] Cerrone, M., et al., Bidirectional ventricular tachycardia and fibrillation elicited in a knock-in mouse model carrier of a mutation in the cardiac ryanodine receptor. Circ Res, 2005. 96(10): p. e77-82.

[124] Cerrone, M., et al., Arrhythmogenic mechanisms in a mouse model of catecholaminergic polymorphic ventricular tachycardia. Circ Res, 2007. 101(10): p. 1039-48.

[125] Kobayashi, S., et al., Dantrolene, a therapeutic agent for malignant hyperthermia, inhibits catecholaminergic polymorphic ventricular tachycardia in a RyR2(R2474S/+) knock-in mouse model. Circ J, 2010. 74(12): p. 2579-84.

[126] Kannankeril, P.J., et al., Mice with the R176Q cardiac ryanodine receptor mutation exhibit catecholamine-induced ventricular tachycardia and cardiomyopathy. Proc Natl Acad Sci U S A, 2006. 103(32): p. 12179-84.

[127] van Oort, R.J., et al., Accelerated development of pressure overload-induced cardiac hypertrophy and dysfunction in an RyR2-R176Q knockin mouse model. Hypertension, 2010. 55(4): p. 932-8.

[128] Mathur, N., et al., Sudden infant death syndrome in mice with an inherited mutation in RyR2. Circ Arrhythm Electrophysiol, 2009. 2(6): p. 677-85.

[129] Liang, X., et al., Impaired interaction between skeletal ryanodine receptors in malignant hyperthermia. Integr Biol (Camb), 2009. 1(8-9): p. 533-9.

[130] Hamilton, S.L. and Serysheva, II, Ryanodine receptor structure: progress and challenges. J Biol Chem, 2009. 284(7): p. 4047-51.

[131] Wagenknecht, T. and M. Samso, Three-dimensional reconstruction of ryanodine receptors. Front Biosci, 2002. 7: p. d1464-74.

[132] Samso, M., et al., Coordinated movement of cytoplasmic and transmembrane domains of RyR1 upon gating. PLoS Biol, 2009. 7(4): p. e85.

[133] Samso, M., X. Shen, and P.D. Allen, Structural characterization of the RyR1-FKBP12 interaction. J Mol Biol, 2006. 356(4): p. 917-27.

[134] Samso, M., T. Wagenknecht, and P.D. Allen, Internal structure and visualization of transmembrane domains of the RyR1 calcium release channel by cryo-EM. Nat Struct Mol Biol, 2005. 12(6): p. 539-44.

[135] Radermacher, M., et al., Cryo-electron microscopy and three-dimensional reconstruction of the calcium release channel/ryanodine receptor from skeletal muscle. J Cell Biol, 1994. 127(2): p. 411-23.

[136] Radermacher, M., et al., Cryo-EM of the native structure of the calcium release channel/ryanodine receptor from sarcoplasmic reticulum. Biophys J, 1992. 61(4): p. 936-40.

[137] Sharma, M.R., et al., Three-dimensional structure of ryanodine receptor isoform three in two conformational states as visualized by cryo-electron microscopy. J Biol Chem, 2000. 275(13): p. 9485-91.

[138] Sharma, M.R., et al., Cryoelectron microscopy and image analysis of the cardiac ryanodine receptor. J Biol Chem, 1998. 273(29): p. 18429-34.

[139] Serysheva, II, et al., Subnanometer-resolution electron cryomicroscopy-based domain models for the cytoplasmic region of skeletal muscle RyR channel. Proc Natl Acad Sci U S A, 2008. 105(28): p. 9610-5.

[140] Serysheva, II, et al., Electron cryomicroscopy and angular reconstitution used to visualize the skeletal muscle calcium release channel. Nat Struct Biol, 1995. 2(1): p. 18-24.

[141] Ludtke, S.J., et al., The pore structure of the closed RyR1 channel. Structure, 2005. 13(8): p. 1203-11.

[142] Wright, N.T., et al., S100A1 and calmodulin compete for the same binding site on ryanodine receptor. J Biol Chem, 2008. 283(39): p. 26676-83.

[143] Maximciuc, A.A., et al., Complex of calmodulin with a ryanodine receptor target reveals a novel, flexible binding mode. Structure, 2006. 14(10): p. 1547-56.

[144] Amador, F.J., et al., Crystal structure of type I ryanodine receptor amino-terminal - trefoil domain reveals a disease-associated mutation "hot spot" loop. Proceedings of the National Academy of Sciences, 2009. 106(27): p. 11040-11044.

[145] Lobo, P.A. and F. Van Petegem, Crystal structures of the N-terminal domains of cardiac and skeletal muscle ryanodine receptors: insights into disease mutations. Structure, 2009. 17(11): p. 1505-14.

[146] Tung, C.C., et al., The amino-terminal disease hotspot of ryanodine receptors forms a cytoplasmic vestibule. Nature, 2010. 468(7323): p. 585-8.

[147] Lobo, P.A., et al., The deletion of exon 3 in the cardiac ryanodine receptor is rescued by beta strand switching. Structure, 2011. 19(6): p. 790-8.

[148] Yuchi, Z., K. Lau, and F. Van Petegem, Disease mutations in the ryanodine receptor central region: crystal structures of a phosphorylation hot spot domain. Structure, 2012. 20(7): p. 1201-11.

[149] Kimlicka, L. and F. Petegem, The structural biology of ryanodine receptors. Science China Life Sciences, 2011. 54(8): p. 712-724.

[150] Shen, Y. and L. Tong, Structural evidence for direct interactions between the BRCT domains of human BRCA1 and a phospho-peptide from human ACC1. Biochemistry, 2008. 47(21): p. 5767-73.

[151] Revel, J.P., The sarcoplasmic reticulum of the bat cricothroid muscle. J Cell Biol, 1962. 12: p. 571-88.

[152] Franzini-Armstrong, C., STUDIES OF THE TRIAD : I. Structure of the Junction in Frog Twitch Fibers. J Cell Biol, 1970. 47(2): p. 488-99.

[153] Campbell, K.P., C. Franzini-Armstrong, and A.E. Shamoo, Further characterization of light and heavy sarcoplasmic reticulum vesicles. Identification of the 'sarcoplasmic reticulum feet' associated with heavy sarcoplasmic reticulum vesicles. Biochim Biophys Acta, 1980. 602(1): p. 97-116.

[154] Franzini-Armstrong, C., Membrane particles and transmission at the triad. Fed Proc, 1975. 34(5): p. 1382-9.

[155] Franzini-Armstrong, C., Structure of sarcoplasmic reticulum. Fed Proc, 1980. 39(7): p. 2403-9.

[156] Bonilla, E., Staining of transverse tubular system of skeletal muscle by tannic acid-glutaraldehyde fixation. J Ultrastruct Res, 1977(2): p. 162-5.

[157] Somlyo, A.V., Bridging structures spanning the junctioning gap at the triad of skeletal muscle. J Cell Biol, 1979. 80(3): p. 743-50.

[158] Ferguson, D.G., H.W. Schwartz, and C. Franzini-Armstrong, Subunit structure of junctional feet in triads of skeletal muscle: a freeze-drying, rotary-shadowing study. J Cell Biol, 1984. 99(5): p. 1735-42.

[159] Saito, A., et al., Preparation and morphology of sarcoplasmic reticulum terminal cisternae from rabbit skeletal muscle. J Cell Biol, 1984. 99(3): p. 875-85.

[160] Saito, A., et al., Ultrastructure of the calcium release channel of sarcoplasmic reticulum. J Cell Biol, 1988. 107(1): p. 211-9.

[161] Yin, C.C. and F.A. Lai, Intrinsic lattice formation by the ryanodine receptor calcium-release channel. Nat Cell Biol, 2000. 2(9): p. 669-71.

[162] Yin, C.C., et al., Two-dimensional crystallization of the ryanodine receptor Ca2+ release channel on lipid membranes. J Struct Biol, 2005. 149(2): p. 219-24.

[163] Orlova, E.V., et al., Two structural configurations of the skeletal muscle calcium release channel. Nat Struct Biol, 1996. 3(6): p. 547-52.

[164] Serysheva, I.I., et al., Subnanometer-resolution electron cryomicroscopy-based domain models for the cytoplasmic region of skeletal muscle RyR channel. Proceedings of the National Academy of Sciences, 2008. 105(28): p. 9610-9615.

[165] Du, G.G., et al., Topology of the Ca2+ release channel of skeletal muscle sarcoplasmic reticulum (RyR1). Proc Natl Acad Sci U S A, 2002. 99(26): p. 16725-30.

[166] Serysheva, II, et al., Structure of the skeletal muscle calcium release channel activated with Ca2+ and AMP-PCP. Biophys J, 1999. 77(4): p. 1936-44.

[167] Liu, Z., et al., Three-dimensional reconstruction of the recombinant type 3 ryanodine receptor and localization of its amino terminus. Proc Natl Acad Sci U S A, 2001. 98(11): p. 6104-9.

[168] Wang, R., et al., Localization of an NH(2)-terminal disease-causing mutation hot spot to the "clamp" region in the three-dimensional structure of the cardiac ryanodine receptor. J Biol Chem, 2007. 282(24): p. 17785-93.

[169] Paul-Pletzer, K., et al., Probing a putative dantrolene-binding site on the cardiac ryanodine receptor. Biochem J, 2005. 387(Pt 3): p. 905-9.

[170] Liu, Z., et al., Localization of a disease-associated mutation site in the three-dimensional structure of the cardiac muscle ryanodine receptor. J Biol Chem, 2005. 280(45): p. 37941-7.

[171] Ikemoto, N. and T. Yamamoto, Regulation of calcium release by interdomain interaction within ryanodine receptors. Front Biosci, 2002. 7: p. d671-83.

[172] Murayama, T., et al., Further characterization of the type 3 ryanodine receptor (RyR3) purified from rabbit diaphragm. J Biol Chem, 1999. 274(24): p. 17297-308.

[173] Benacquista, B.L., et al., Amino acid residues 4425-4621 localized on the three-dimensional structure of the skeletal muscle ryanodine receptor. Biophys J, 2000. 78(3): p. 1349-58.

[174] Liu, Z., et al., Three-dimensional reconstruction of the recombinant type 2 ryanodine receptor and localization of its divergent region 1. J Biol Chem, 2002. 277(48): p. 46712-9.

[175] Liu, Z., et al., Location of divergent region 2 on the three-dimensional structure of cardiac muscle ryanodine receptor/calcium release channel. J Mol Biol, 2004. 338(3): p. 533-45.

[176] Zhang, J., et al., Three-dimensional localization of divergent region 3 of the ryanodine receptor to the clamp-shaped structures adjacent to the FKBP binding sites. J Biol Chem, 2003. 278(16): p. 14211-8.

[177] Jones, P.P., et al., Localization of PKA phosphorylation site, Ser(2030), in the three-dimensional structure of cardiac ryanodine receptor. Biochem J, 2008. 410(2): p. 261-70.

[178] Meng, X., et al., Three-dimensional localization of serine 2808, a phosphorylation site in cardiac ryanodine receptor. J Biol Chem, 2007. 282(35): p. 25929-39.

[179] Wagenknecht, T., et al., Cryoelectron microscopy resolves FK506-binding protein sites on the skeletal muscle ryanodine receptor. Biophys J, 1996. 70(4): p. 1709-15.

[180] Wagenknecht, T., et al., Locations of calmodulin and FK506-binding protein on the three-dimensional architecture of the skeletal muscle ryanodine receptor. J Biol Chem, 1997. 272(51): p. 32463-71.

[181] Sharma, M.R., et al., Three-dimensional visualization of FKBP12.6 binding to an open conformation of cardiac ryanodine receptor. Biophys J, 2006. 90(1): p. 164-72.

[182] Wagenknecht, T., et al., Localization of calmodulin binding sites on the ryanodine receptor from skeletal muscle by electron microscopy. Biophys J, 1994. 67(6): p. 2286-95.

[183] Samso, M. and T. Wagenknecht, Apocalmodulin and Ca2+-calmodulin bind to neighboring locations on the ryanodine receptor. J Biol Chem, 2002. 277(2): p. 1349-53.

[184] Meng, X., et al., CLIC2-RyR1 interaction and structural characterization by cryo-electron microscopy. J Mol Biol, 2009. 387(2): p. 320-34.

[185] Samso, M., et al., Three-dimensional location of the imperatoxin A binding site on the ryanodine receptor. J Cell Biol, 1999. 146(2): p. 493-9.

[186] Zhou, Q., et al., Structural and functional characterization of ryanodine receptor-natrin toxin interaction. Biophys J, 2008. 95(9): p. 4289-99.

[187] Bhuiyan, Z.A., et al., Expanding spectrum of human RYR2-related disease: new electrocardiographic, structural, and genetic features. Circulation, 2007. 116(14): p. 1569-76.

[188] Marjamaa, A., et al., Search for cardiac calcium cycling gene mutations in familial ventricular arrhythmias resembling catecholaminergic polymorphic ventricular tachycardia. BMC Med Genet, 2009. 10: p. 12.

[189] Garzon, J.I., et al., ADP_EM: fast exhaustive multi-resolution docking for high-throughput coverage. Bioinformatics, 2007. 23(4): p. 427-33.

[190] Chacon, P. and W. Wriggers, Multi-resolution contour-based fitting of macromolecular structures. J Mol Biol, 2002. 317(3): p. 375-84.

[191] Wriggers, W. and P. Chacon, Modeling tricks and fitting techniques for multiresolution structures. Structure, 2001. 9(9): p. 779-88.

[192] Seo, M.D., et al., Structural and functional conservation of key domains in InsP3 and ryanodine receptors. Nature, 2012. 483(7387): p. 108-12.

[193] Marx, S.O., et al., PKA phosphorylation dissociates FKBP12.6 from the calcium release channel (ryanodine receptor): defective regulation in failing hearts. Cell, 2000. 101(4): p. 365-76.

[194] Wehrens, X.H., et al., Ryanodine receptor/calcium release channel PKA phosphorylation: a critical mediator of heart failure progression. Proc Natl Acad Sci U S A, 2006. 103(3): p. 511-8.

[195] Wehrens, X.H., et al., Ca2+/calmodulin-dependent protein kinase II phosphorylation regulates the cardiac ryanodine receptor. Circ Res, 2004. 94(6): p. e61-70.

[196] Jiang, M.T., et al., Abnormal Ca2+ release, but normal ryanodine receptors, in canine and human heart failure. Circ Res, 2002. 91(11): p. 1015-22.

[197] Zhang, H., et al., Hyperphosphorylation of the cardiac ryanodine receptor at serine 2808 is not involved in cardiac dysfunction after myocardial infarction. Circ Res, 2012. 110(6): p. 831-40.

[198] Sharma, P., et al., Structural Determination of the Phosphorylation Domain of the Ryanodine Receptor. FEBS J, 2012.

[199] Mackrill, J.J., Ryanodine Receptor Calcium Release Channels: An Evolutionary Perspective. 2012. 740: p. 159-182.

[200] van de Graaf, S.F., et al., Identification of BSPRY as a novel auxiliary protein inhibiting TRPV5 activity. J Am Soc Nephrol, 2006. 17(1): p. 26-30.

[201] Cui, Y., et al., A dihydropyridine receptor alpha1s loop region critical for skeletal muscle contraction is intrinsically unstructured and binds to a SPRY domain of the type 1 ryanodine receptor. Int J Biochem Cell Biol, 2009. 41(3): p. 677-86.

[202] Kelley, L.A. and M.J. Sternberg, Protein structure prediction on the Web: a case study using the Phyre server. Nat Protoc, 2009. 4(3): p. 363-71.

[203] Mackrill, J.J., Ryanodine receptor calcium release channels: an evolutionary perspective. Adv Exp Med Biol, 2012. 740: p. 159-82.

IntechOpen